Structural studies of ligand-protein complex: the importance of structural change for drug design

Aiko Fujino-Nakajima

Teijin Pharma Limited
Institute for Bio-medical Research
Japan

2013

CONTENTS

Chapter 2

Crystal structure of human cyclin-dependent kinase-2 complex with MK2 inhibitor TEI-I01800: insight into the selectivity

Chapter 3

Structure of the β-form of human MK2 in complex with the non-selective kinase inhibitor TEI-L03090

General Introduction

Mitogen activated protein kinase (MAPK) pathway is a signaling pathway constituted with three kinds of protein phosphorylated enzymes (kinase) called MAPKKK, MAPKK, and MAPK. It is a basic intracellular communication system common to all the eukaryotic organisms. In the mammalian cells, there are at least four kinds of MAPK pathways called ERK1/2, ERK5, JNK/SAPK and p38 of which the physiological function is different from each other. Among these, the p38 MAPK signaling pathway, which is activated by the DNA damage, the oxidative stress, the infection of inflammatory cytokine and a pathogenic organ, has played the central role in control of immunoreaction or inflammation.

Figure 0-1 shows the p38 MAPK signaling pathway (Guess *et al*., *PLoS One*. 2013, **8**, e54239).

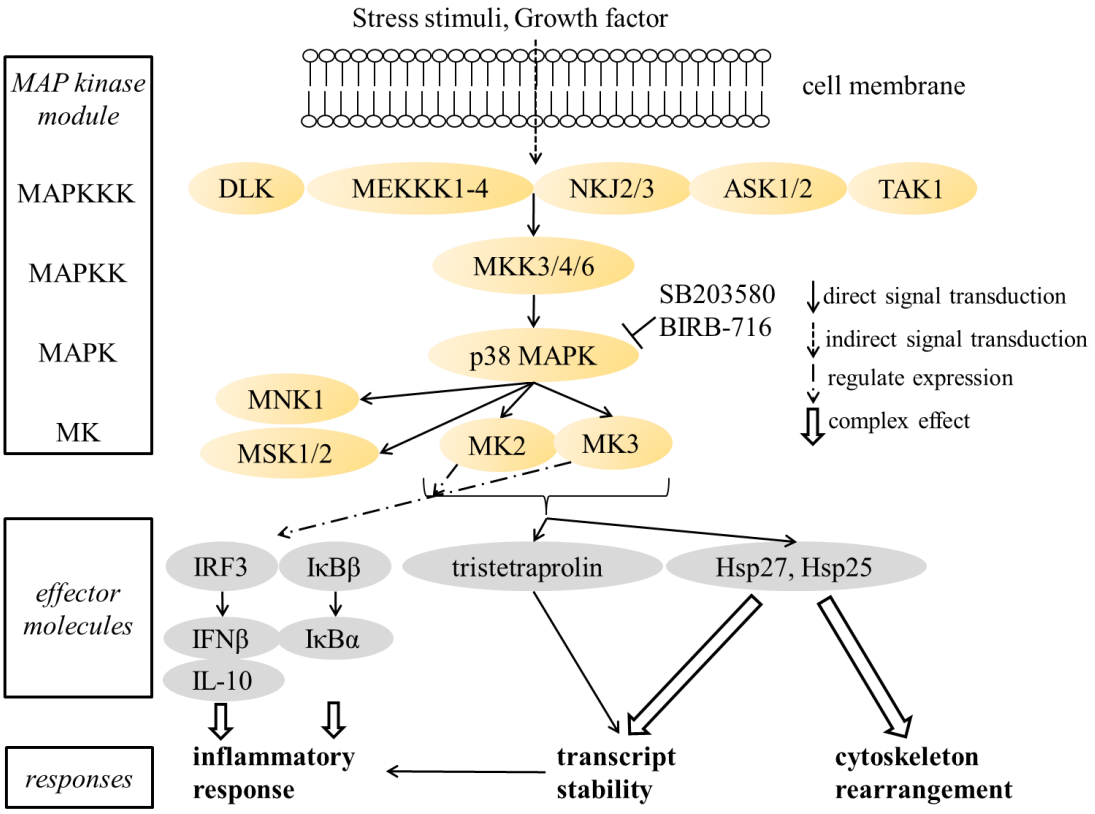

Figure 0-1 The p38 MAPK signaling pathway.

MK2 is a downstream kinase of p38 MAPK and directly phosphorylated by p38 MAPK.

P38 MAPKs (α, β) are phosphorylated by MKK3/4/6 which is a member of MEKK. P38 MAPK is also involved in the phosphorylation of mitogen activate protein kinase activate kinase-2 (MK2 or MAPKAPK-2), MK3 (MAPKAP-K3), MNK1, MSK1/2 and the control of several transcription factors such as activating transcription factor-2 (ATF-2), signal transducers and activator of transcription 1 (Stat1), Myc/Max complex, and so on. SB203580 or BIRB-716 which is a specific inhibitor of p38 MAPKα/β suppresses the phosphorylation of p38 MAPK and production of inflammatory cytokine, such as Interleukin (IL)-1β, tumor necrosis factor (TNF)-α, matrix metalloproteinase-2 (MMP-2) and MMP-9 by administration to mice. Since TNF-α causes many types of inflammatory diseases such as rheumatoid arthritis and Chron's disease, the anti-TNF-α antibodies such as infliximab are used as effective medicines. However,

biological drugs have several problems such as a high cost, a risk of infection and a patient's burden to injection. Therefore, anti-TNF-α drug which can be administered orally is needed. Several kinases inhibitors in p38 MAPK signaling pathway are being developed for anti-inflammatory diseases. Especially p38 MAPK inhibitors are studied a lot and the clinical trials of p38 MAPK inhibitors have run before. However, the results were unsuccessful because of the side-effects caused by blocking another response controlled by p38 MAPK (Fig.0-2).

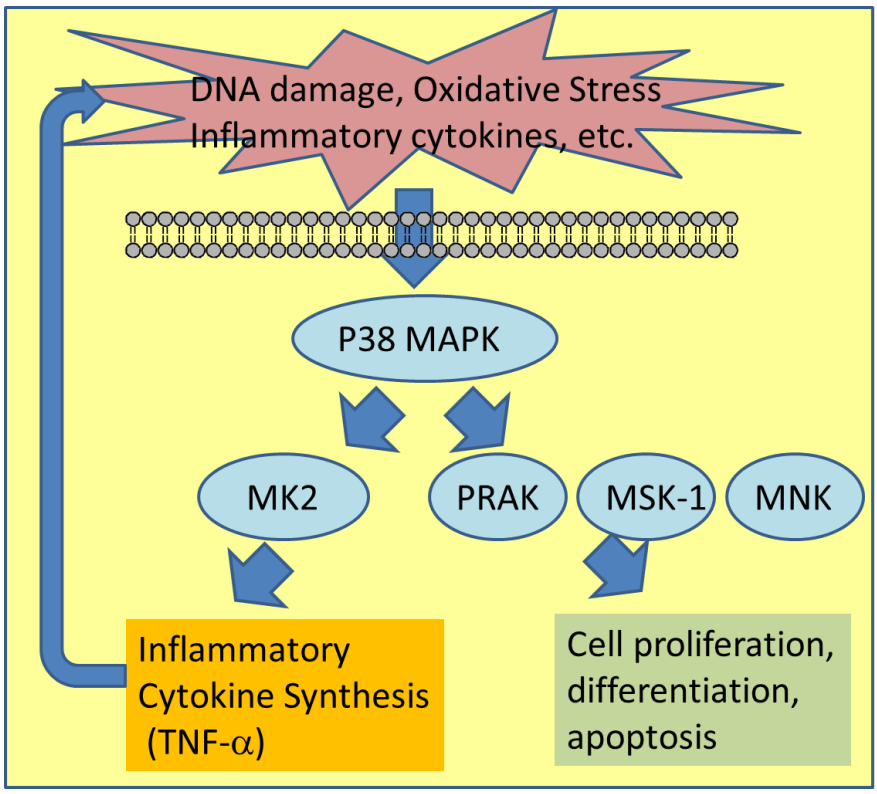

Figure 0-2 p38 MAPK signaling pathway and MK2

Although p38 MAPK controls not only inflammatory cytokine synthesis but also cell cycle, MK2 controls only cytokine biosynthesis.

MK2 (uniprot accession number: P49137), which is a Ser/Thr kinase activated by the phosphorylation of Ser272, Thr222 and Thr334 residues, and it is about 45 kDa protein composed of 400 amino acids. In 1999 based on the experimental result that showed MK2-knockout mice has a reduced level of production of cytokines such as TNF-α, interferon-γ, IL-1β and IL-6, it was indicated that MK2 is an essential component in the inflammatory response which regulates TNF-α biosynthesis (Kotlyarov *et al*., *Nat. Cell Biol*. 1999, **1**, 94–97], and it has been considered a novel target for the development of new small-molecule drugs for oral administration. Because MK2 is a downstream kinase of p38 MAPK and controls only cytokine biosynthesis, MK2 inhibitor is considered safer than other p38 MAPK inhibitors.

However, the detailed mechanism of the TNF-α biosynthesis has been unknown. Recently it was reported that both MK2 and MK3 regulate an inflammatory response intricately by direct or through a transcript stability (Guess *et al*., *PLoS One*. 2013, **8**, e54239).

There are more than 500 kinases in the human genome, and they are key controllers of cell behavior (Manning *et al*., *Science*. 2002, **298**, 1912-1934). Their overall structures called kinase fold are highly conserved in the protein kinase family, and several non-selective inhibitors bound to their ATP-binding pockets are found. In the case of development of kinase inhibitors, to avoid the side-effects of drugs, the selectivity of target kinase over other kinases is most important. Therefore, when the target kinase was selected, we should set the antitargets to prevent undesirable side-effects. The antitargets are different depending on the main targets because the drugs certainly have some side-effects and the balances between main effects and side-effects are significant. Especially, the drugs used chronically for anti-inflammatory diseases need high safety level, so the kinases which control normal cell behavior like cell growth and apoptosis are considered to be antitargets.

In our laboratory, at the beginning of 2000s the MK2 inhibitor program for the anti-inflammatory therapy, such as rheumatoid arthritis was started. At the time, the crystal structure of MK2 was unknown and we started to try to solve the crystal structure of MK2–inhibitor complex. Because the crystal of MK2–inhibitor complex was not obtained easily, we

tried to make a several truncated mutants, tag fused proteins and expression systems. On the other hand, structure based drug design (SBDD) is performed using cyclin-dependent kinase 2 (CDK2)–inhibitor docking model because MK2 structure has not been solved and the initial hit compound showed more potent inhibition for CDK2 than MK2.

CDK2 (uniprot accession number: P24941) is also a Ser/Thr kinase, which is about 33 kDa protein composed of 298 amino acids, and the active complexes with a specific cyclin molecule control the cell cycle (Fig.0-3; Tsai *et al*., *Nature*. 1991, **353**, 174–177).

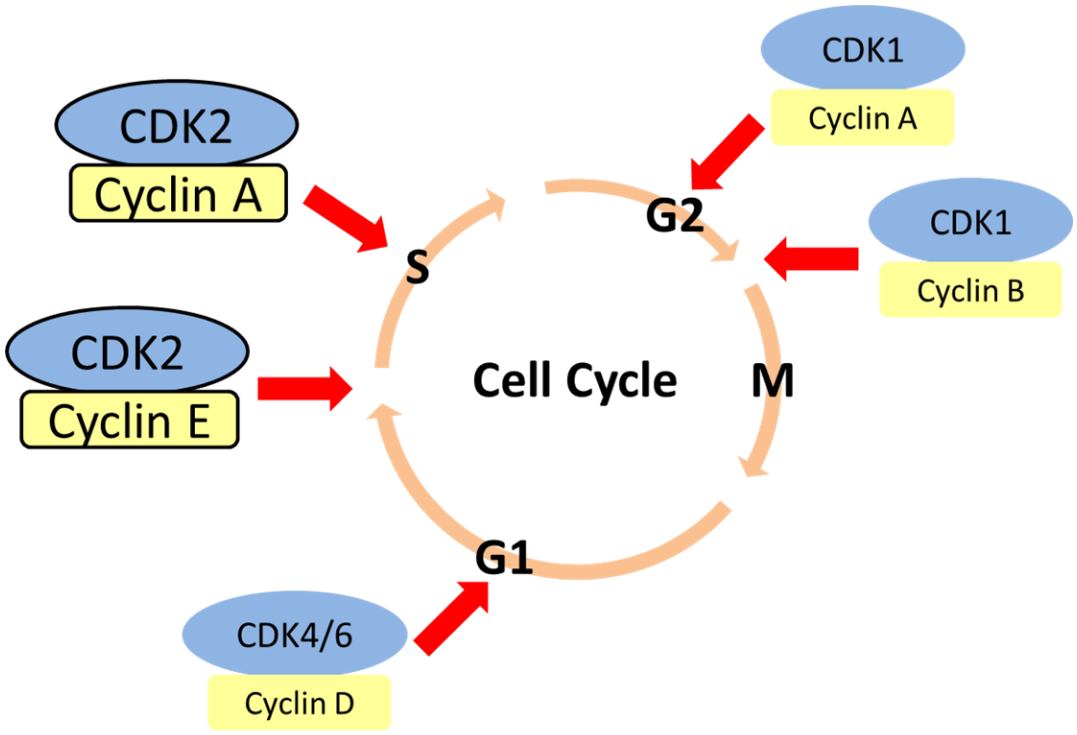

Figure 0-3 Cell cycle and CDKs.

Because the interference with the cell cycle via the inhibition is likely to be an undesirable feature in chronic anti-inflammatory drugs, we especially focused on the selectivity of MK2 inhibitor over CDK2 in our program. The sequence identity and similarity between MK2 and CDK2 were 14.9% and 30.3% respectively, but the sequence similarity of ATP-binding site was higher than other regions. Therefore, we selected CDK2 as an antitarget kinase and determined the crystal structure of CDK2 in complex with our MK2 inhibitors in order to understand the binding interaction and to develop the MK2 selective inhibitor.

In 2002 the first crystal structure of apo-MK2, and next year MK2–ADP and staurosporine complexes were reported (Meng *et al*., *J. Biol. Chem*. 2002, **277**, 37401–37405; Underwood *et al*., *Structure*. 2003, **11**, 627–636). We continued to try to solve the MK2–our inhibitor complex after that. In 2004, the first MK2 structure in complex with our inhibitor TEI-I01800 was determined and it revealed really an unpredictable structure. A wide variety of MK2 inhibitors with various properties were designed based on MK2–TEI-I01800 structure; the details of progress of our MK2 inhibitors are described in Kosugi *et al*., *J. Med. Chem*. 2012, **55**, 6700–6715. Among them, TEI-I01800 is one of the most promising inhibitors, showing good potency and selectivity for CDK2 and other kinases.

In this thesis, in chapter 1, we report the crystal structure of MK2 in complex with MK2 selective inhibitor TEI-I01800 and the novel structural change of the Gly-rich loop from β-sheet to α-helix, which is commonly observed as β-sheet in the kinase family enzymes. In chapter 2, the crystal structure of CDK2–TEI-I01800 complex and the mechanism of kinase selectivity, and in chapter 3, the crystal structure of MK2 in complex with the non-selective inhibitor TEI-L03090 to support our hypothesis of structural change of Gly-rich loop are described, respectively. These results demonstrate that a stable conformer of TEI-I01800 can change the secondary structure of Gly-rich loop of MK2 and create the specific binding pocket suitable for the binding. This is the most important factor for selectivity for CDK2 and other kinases.

Chapter 1

Structural analysis of an MK2–inhibitor complex: insight into the regulation of the secondary structure of the Gly-rich loop by TEI-I01800

Summary

Mitogen-activated protein kinase-activated protein kinase 2 (MAPKAP-K2 or MK2) is a Ser/Thr kinase from the p38 mitogen-activated protein kinase signaling pathway and plays an important role in inflammatory diseases. The crystal structure of the complex of human MK2 (residues 41–364) with the potent MK2 inhibitor TEI-I01800 (p*K*i = 6.9) was determined at 2.9 Å resolution. The MK2 structure in the MK2–TEI-I01800 complex is composed of two domains, as observed for other Ser/Thr kinases; however, the Gly-rich loop in the N-terminal domain forms an α-helix structure and not a β-sheet. TEI-I01800 binds to the ATP-binding site as well as near the substrate-binding site of MK2. Both TEI-I01800 molecules have a non-planar conformation that differs from those of other MK2 inhibitors deposited in the RCSB Protein Data Bank. The MK2‑TEI-I01800 complex structure is the first active MK2 with an α-helical Gly-rich loop and TEI-I01800 regulates the secondary structure of the Gly-rich loop.

1 Introduction

Mitogen-activated protein kinase-activated protein kinase 2 (MAPKAP-K2 or MK2) is a Ser/Thr kinase from the p38 mitogen-activated protein (MAP) kinase signaling pathway. The p38 MAP kinase pathway plays an important role in the production of TNF-α and various cytokines (Beyaert *et al*., 1996). TNF-α causes many types of inflammatory diseases such as rheumatoid arthritis, for which anti-TNF-α antibodies such as Infliximab are the most effective medications. TNF-α is thus a promising target for anti-inflammatory therapy.

The p38 MAP kinase inhibitors SB203580 and BIRB-796 inhibit LPS-induced cytokine synthesis (Lee *et al*., 1994; Pargellis *et al*., 2002; Gruenbaum *et al*., 2009) and also prevent phosphorylation and activation of MK2 (Cuenda *et al*., 1995). As MK2-knockout mice showed a reduction in TNF-α, interferon-γ, IL-1β and IL-6, MK2 was shown to be essential for LPS-induced TNF-α biosynthesis (Kotlyarov *et al*., 1999). MK2 plays an important role in TNF-α biosynthesis and is a novel target for the development of new small-molecule drugs for oral administration. Several pharmaceutical companies have reported new small-molecule inhibitors of MK2 (Hillig *et al*., 2007; Anderson *et al*., 2007, 2009; Wu *et al*., 2007; Goldberg *et al*., 2008; Xiong *et al*., 2008; Argiriadi *et al*., 2009).

The apo structure of MK2 was first determined in 2002 (Meng *et al*., 2002) and the structures of the MK2–AMP-PNP (Kurumbail *et al*., 2003), MK2–ADP and MK2–staurosporine complexes were determined in 2003 (Underwood *et al*., 2003). Several structures of MK2 in complex with small molecule inhibitors have been reported and their structure activity relationships have been discussed (Hillig *et al*., 2007; Anderson *et al*., 2007, 2009; Wu *et al*., 2007). Both the apo–MK2 and the MK2–AMP-PNP structures represent inactive conformations (with the Lys93–Glu104 salt bridge disrupted). Apo–MK2 has an α-helical Gly-rich loop (α-form), while MK2–AMP-PNP has a β-sheet Gly-rich loop (β-form). In contrast, the structures of the complexes of active MK2 (amino-acid residues 41–364 or 45–371) with ADP, staurosporine and various small molecule inhibitors all have the β-form. Although these constructs contain part of the auto-inhibitory domain sequence that associates with the

substrate-binding region, these sequences are disordered. In particular, the 41–364 construct of MK2 has been reported to be constitutively active without phosphorylation by p38 MAP kinase (Underwood *et al*., 2003). Therefore, the α-form of apo–MK2 was considered to be an artificial structure that was produced as an effect of mercury modification (Underwood *et al*., 2003). However, the secondary structure of the Gly-rich loop of active MK2 has not been focused on in previous reports on MK2 and other kinases.

In the present study, we determined the structure of human MK2 in complex with the potent inhibitor TEI-I01800 at 2.9 Å resolution. The results showed that the Gly-rich loop of the MK2–TEI-I01800 complex formed an α-helix and differs from other reported MK2–small-molecule inhibitor complexes. Here, we report the crystal structure of the MK2–TEI-I01800 complex and suggest that the structural features of TEI-I01800 are important in regulating the secondary structure of the Gly-rich loop.

2 Materials and methods

2.1 Cloning, expression and purification

The expression plasmids were constructed as described by Underwood *et al*. (2003). The human MK2 kinase domain (residues 41–364) was amplified by PCR using oligonucleotide primers, inserted between the *Nde*I and *Xho*I sites of pET-22b(+) (Novagen) and then transformed into *Escherichia coli* strain BL21 (DE3) (Novagen). These cultures were grown to an OD600 of 0.7 and expression was carried out in LB medium containing 100 µg ml^{-1} ampicillin with 1 m*M* isopropyl-β-D-1-thiogalactoside (IPTG) at 298 K for about 3 hours. The cell pellets from 500 ml culture were suspended in 50 ml buffer *A* (20 m*M* HEPES pH 7.5, 10 m*M* NaCl and 5 m*M* DTT) and sonicated on ice. The supernatant was applied onto a Q Sepharose HP column (GE Healthcare) and the flow-through sample was collected. The solution containing MK2 protein was applied onto a Resource S column (GE Healthcare) and eluted using a linear gradient to buffer *B* (20 m*M* HEPES pH 7.5, 500 m*M* NaCl and 5 m*M* DTT). The fraction containing MK2 was applied onto a Superdex 75 gel-filtration column (GE Healthcare) equilibrated with buffer *C* (20 m*M* HEPES pH 7.5, 200 m*M* NaCl and 5 m*M* DTT) and the fractions containing a single peak were collected. The purified human MK2 was concentrated to 5–20 mg ml^{-1} in buffer *D* (20 m*M* HEPES pH 7.5, 5 m*M* $MgCl_2$, 200 m*M* NaCl and 10 m*M* DTT) before crystallization.

2.2 Crystallization and data collection

The kinase domain of MK2 is known to be a difficult crystallization target and all MK2 crystals described to date diffracted to only low or medium resolution (Meng *et al*., 2002; Kurumbail *et al*., 2003; Underwood *et al*., 2003; Hillig *et al*., 2007; Anderson *et al*., 2007, 2009; Wu *et al*., 2007; Goldberg *et al*., 2008; Xiong *et al*., 2008; Argiriadi *et al*., 2009). The first MK2–TEI-I01800 crystal was obtained under similar conditions to those reported previously (Underwood *et al*., 2003). However, it diffracted to low resolution and was predicted to belong to space group $P2_12_12_1$ with 12 molecules in the asymmetric unit. Therefore, co-crystallizations were performed using commercially available screening kits consisting of more than 1000

conditions and soaking using both apo–MK2 and MK2–ADP. Several crystals were obtained in various conditions, but they all diffracted to low resolution and belonged to the same space group with similar unit-cell parameters. Optimized MK2–TEI-I01800 crystals were obtained by the co-crystallization method and were grown in 0.1 *M* HEPES pH 7.5, 1.6–2.0 *M* ammonium sulfate and 5% ethanol. All crystallizations were performed at 293 K using the sitting-drop vapour-diffusion method. After soaking in cryoprotectant buffer containing 30% sucrose, a data set was collected at 100 K on the SPring-8 BL32B2 beamline using an R-AXIS IV image-plate detector. The MK2–TEI-I01800 crystals diffracted to less than 2.9 Å resolution and belonged to space group $P2_12_12_1$, with unit-cell parameters a = 139.15, b = 180.95 and c = 216.09 Å and 12 molecules in the asymmetric unit (Matthews coefficient V_M = 3.03 $Å^3$ Da^{-1}, solvent content V_{solv} = 59.3%). The reflection data were processed using the *HKL*-2000 software package (Otwinowski & Minor, 1997). The crystal of MK2–TEI-I01800 is shown in Fig. 1-1 and the data-processing and refinement statistics are shown in Table 1-1.

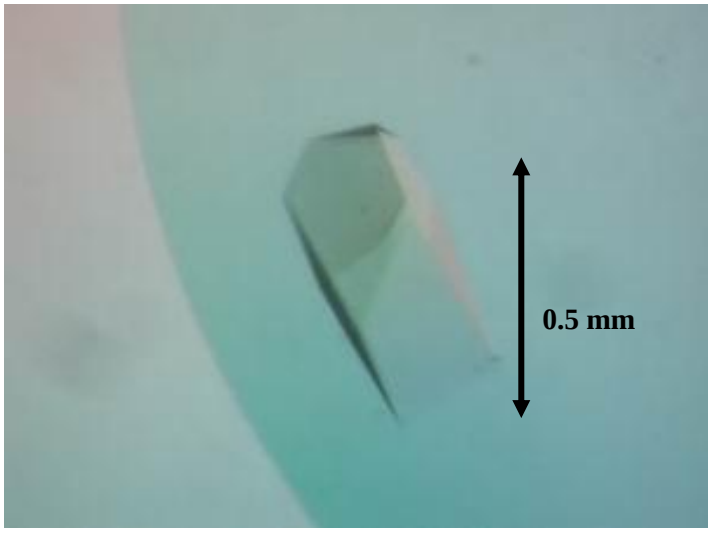

Figure 1-1 Crystal of MK2–TEI-I01800.

	MK2–TEI-I01800
Data collection	
Beam line	SPring-8 BL32B2
Wave length (Å)	1.000
Resolution (Å)	50.0-2.90 (3.00-2.90)
Mosaicity (°)	0.32
No. of unique reflections	121109
R_{merge} (%)	9.1 (44.7)
Completeness (%)	99.8 (99.0)
Multiplicity	5.7 (4.5)
Average $I/\sigma(I)$	24.7 (3.3)
Space group	$P2_12_12_1$
Unit-cell parameters (Å)	
a	139.15
b	180.95
c	216.09
Refinement	
Resolution (Å)	20-2.9
R factor (%)	28.8
R_{free} (%)	33.5
No. of reflections work/test	114397/6068
R.m.s.d. from ideal values	
Bond lengths (Å)	0.012
Bond angles (°)	1.28
Ramachandran plot analysis	
Most favoured regions (%)	87.7
Additional allowed regions (%)	12.0
Generously allowed regions (%)	0.3
Disallowed regions (%)	0.0

Table 1-1 Data-collection and refinement statistics.

Values in parentheses are for the highest resolution shell.

2.3 Structure determination and refinement

Structure determination was performed by molecular replacement using the MK2 protein from the MK2–ADP complex (PDB code 1ny3; Underwood *et al.*, 2003) as a search model. Several programs were used, but only *MOLREP* (Vagin & Teplyakov, 1997) found six of the 12 molecules in the asymmetric unit, with corr(I) = 42.0 and R = 54.7%. However, an $F_o - F_c$ electron-density map calculated with six molecules showed clear positive blobs that were recognizable as MK2 molecules (R = 43.1%, R_{free} = 49.8%). Consequently, after density modification by NCS averaging (Bricogne, 1974; Schuller, 1996) using *DM* (Cowtan, 1994) in the CCP4 suite (Collaborative Computational Project, Number 4, 1994), a further six molecules were assigned manually in the density maps using *QUANTA* (Accelrys Inc.; http://accelrys.com/). In this process, every time a molecule was found rigid-body and restrained refinement were performed using *REFMAC* (Murshudov *et al.*, 1997) to check the R factor and a new electron-density map was calculated. After the determination of 12 MK2 molecules, the R and R_{free} factors fell to 27.9% and 37.6%, respectively. At this stage, the $F_o - F_c$ map clearly showed a positive blob-shaped TEI-I01800 molecule at the ATP-binding site in each molecule; 12 TEI-I01800 molecules were assigned by *QUANTA*/*X-LIGAND* and the R and R_{free} factors fell to 21.5% and 29.4%, respectively. Moreover, positive peaks appeared near the substrate-binding pockets in the $F_o - F_c$ map and an additional 12 TEI-I01800 molecules were assigned as previously. The structure of the MK2–TEI-I01800 complex was then refined to R and R_{free} factors of 20.9% and 29.2%, respectively. We found that both 2 $F_o - F_c$ and $F_o - F_c$ maps showed a different structure around the Gly-rich loop in the current protein model compared with the search model. The Gly-rich loops in 12 molecules were rebuilt based on an OMIT map and structure refinement was continued to R and R_{free} factors of 20.2% and 28.7%, respectively. However, the root-mean-square distance (r.m.s.d.) of the bond lengths and torsion angles from ideal values were very large and were not improved by *REFMAC*. Consequently, after conversion to *CNX* (Accelrys Inc.; http://accelrys.com/) format with the same R_{free} flags, torsion-angle refinement was carried out automatically using the *LAFIRE* program (Yao *et al.*, 2006; Zhou *et al.*, 2006) running with the refinement program *CNX* with NCS restraints. The

final R and R_{free} factors were 28.8% and 33.5%, which were larger than the previous values; however, the r.m.s.d. values and Ramachandran plot analysis were dramatically improved. The coordinates and structure factors have been deposited in the PDB with code 3a2c. Figures were produced using *DS Visualizer* (Accelrys Inc.; http://accelrys.com/).

3 Results and discussion

3.1 Structure of the MK2–TEI-I01800 complex

3.1.1 Overall structure

There are 12 MK2–TEI-I01800 complexes in the asymmetric unit of the $P2_12_12_1$ crystal constituting four trimers (described as chains *ABC*, *DEF*, *GHI* and *JKL*) that form a ring. In a trimer, each molecule interacts with neighboring molecules in the substrate-binding pocket. This crystal-packing and oligomerization state is the same as in the complex of MK2 with the pyrrolopyrimidine analogue compound-1 (Hillig *et al.*, 2007). The r.m.s.d. values on C^{α} atoms between the monomers of MK2–TEI-I01800 are almost the same and are less than 1 Å. Molecule *A*, which has the lowest average *B*-factor, was selected as the monomer structure that is discussed below. The monomer structure of MK2–TEI-I01800 contains two domains (N-terminal and C-terminal domains) as in other kinases and is shown in Fig. 1-2.

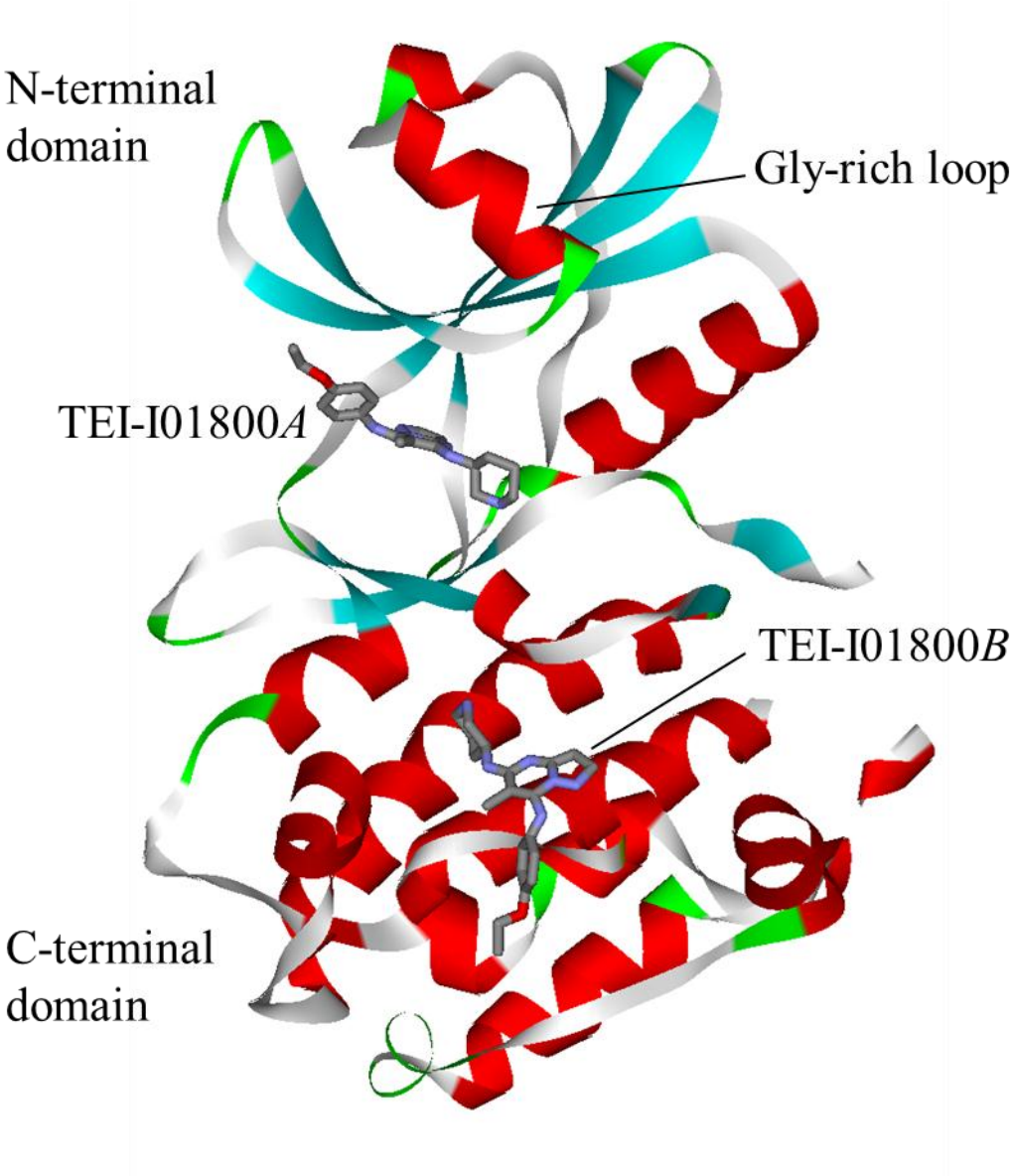

Figure 1-2 Structure of molecule *A* of MK2–TEI-I01800.

The overall kinase fold of MK2 is shown in ribbon representation (α-helices are shown in red, β-sheets in blue and β-turns in green). TEI-I01800*A* bound to MK2 in the ATP-binding site and TEI-I01800*B* bound in the substrate-binding site.

In the MK2–TEI-I01800 complex one MK2 molecule is bound by two TEI-I01800 molecules. The first TEI-I01800 molecule (TEI-I01800*A*) is bound to the ATP-binding site between the N-terminal and C-terminal domains. The second TEI-I01800 molecule (TEI-I01800*B*) interacts with MK2 near the substrate-binding site in the C-terminal domain. Figs. 1-3 and 1-4 show the electron-density maps for TEI-I01800*A* and TEI-I01800*B*, respectively.

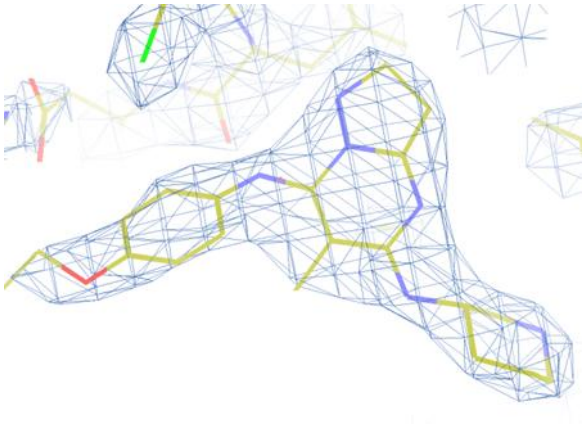

Figure 1-3 2 $F_o - F_c$ maps (contoured at 1.0 σ) of TEI-I01800*A*.

Figure 1-4 2 $F_o - F_c$ maps (contoured at 1.0 σ) of TEI-I01800*B*.

Two inhibitors could be placed in the $F_o - F_c$ map despite the low resolution. The most notable feature of this complex is the Gly-rich loop in the N-terminal domain. In the MK2–TEI-I01800 complex all 12 molecules contain an α-helical Gly-rich loop. The initial density map calculated using the MK2–ADP complex (Underwood *et al.*, 2003) clearly showed a negative $F_o - F_c$ map around the β-sheet Gly-rich loop. Therefore, the corresponding residues were placed in the positive blobs by manual C^{α} tracing. After rebuilding the Gly-rich loop, the secondary structure was similar to that of the α-helical Gly-rich loop of the apo–MK2 structure. The electron-density map for the α-helical Gly-rich loop of molecule *A* is shown in Fig. 1-5.

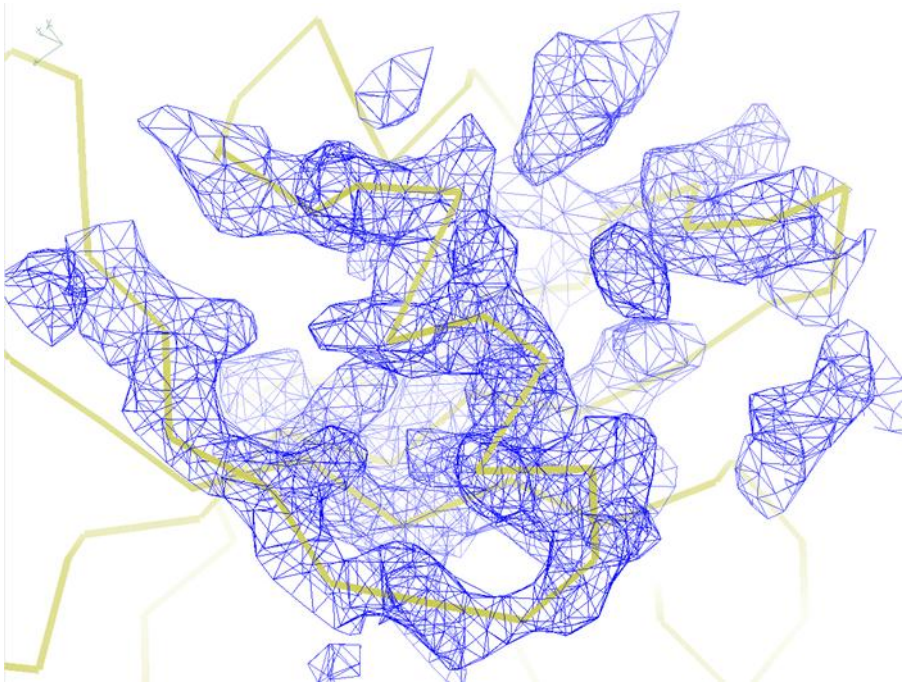

Figure 1-5 $2F_o - F_c$ maps (contoured at 1.0 σ) of the α-helical Gly-rich loop.

The α-helical Gly-rich loop could be placed in the density maps despite the low resolution.

With the exception of the apo–MK2 structure (Meng *et al.*, 2002), the Gly-rich loops of all other MK2s have the β-form. In these structures, each Gly-rich loop covers the ATP-binding site to stabilize ADP, staurosporine and other inhibitors. However, the ATP-binding site in the MK2–

TEI-I01800 complex opens and is larger than that of MK2s with the β-sheet Gly-rich loop.

3.1.2 Binding mode and structure of TEI-I01800

The molecular structure and atomic numbering of TEI-I01800 are shown in Fig. 1-6.

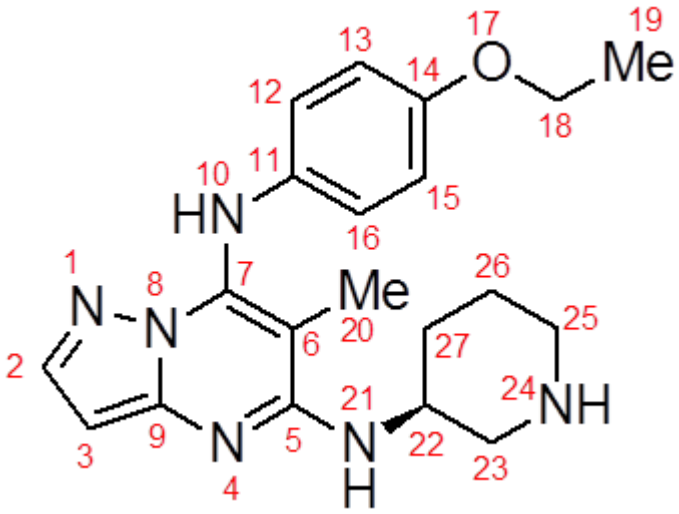

Figure 1-6 Molecular structure of TEI-I01800.

Atom numbers were assigned sequentially. The bonds C7−N10 and N10−C11 between the pyrazolo[1,5-*a*]pyrimidine-scaffold part and the *p*-ethoxyphenyl group at the 7-position are freely rotatable.

It has a pyrazolo[1,5-*a*]pyrimidine scaffold with a (3*S*)-piperidylamino group at the 5-position, a methyl group at the 6-position and a *p*-ethoxyphenylamino group at the 7-position. Its inhibitory activity for MK2 is p*K*i = 6.90. The binding mode of TEI-I01800*A* is shown in Fig. 1-7.

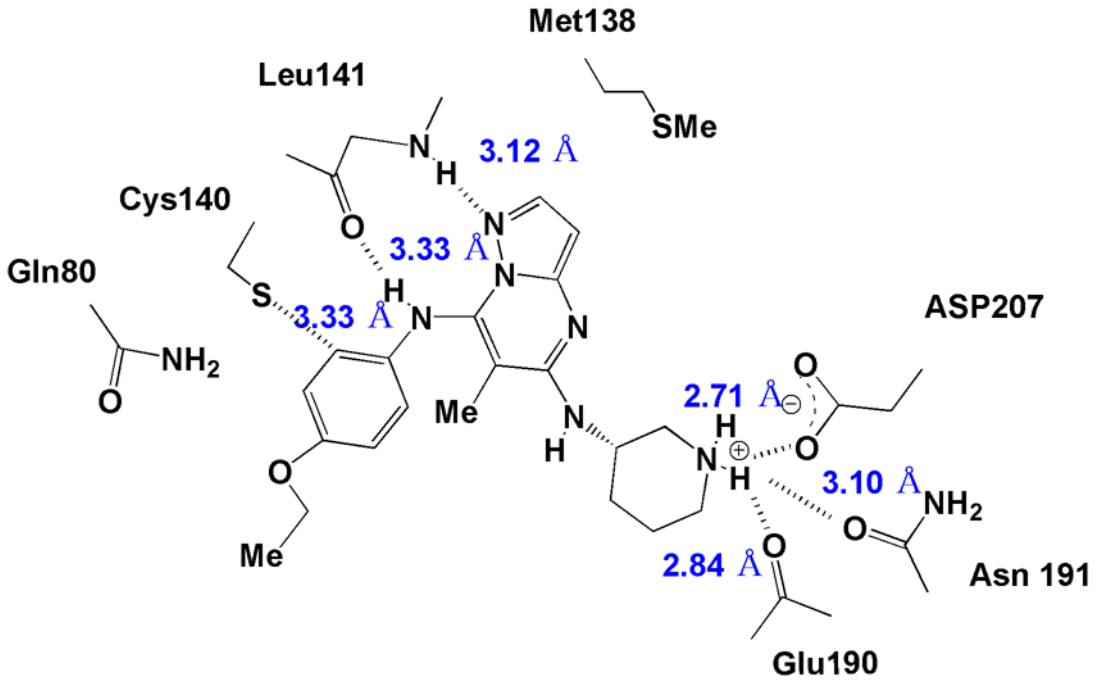

Figure 1-7 Binding interaction of TEI-I01800*A* and MK2.

TEI-I01800*A* interacts with the backbone amide of Leu141 through two hydrogen bonds: TEI-I01800A N1—Leu141 N (3.12 Å) and TEI-I01800A N10—Leu141 oxygen atom (3.33 Å). The N24 atom of TEI-I01800*A* must be ionized by hydrogen bond to the carboxyl group of Asp207 (2.71 Å). This atom also makes two additional hydrogen bonds to the backbone carbonyl oxygen atom of Glu190 (2.84 Å) and OD1 of Asn191 (3.10 Å). The (3*S*)-piperidylamino group is important for the MK2 inhibitory activity of TEI-I01800. Another notable interaction is the van der Waals interaction between C12/C16 of the *p*-ethoxyphenyl group at the 7-position and the sulfate atom of Cys140. This *p*-ethoxyphenyl group is also important for the MK2 inhibitory activity; the inhibitory activity decreased when the *p*-ethoxyphenyl group was removed (unpublished data). As a result of the structural change from β-form to α-form MK2, a new pocket consisting of Leu79, Gln80, Cys140 and Asp142 is exposed and interacts with the *p*-ethoxyphenyl group at the 7-position (shown in Fig. 1-8). In the β-sheet Gly-rich loop structure, part of the β-sheet covers and hides this pocket. However, in the α-form MK2 structure residues ^{65}VTSQVLGLGINGKVLQ^{80} are moved a maximum distance of 13.7 Å (for the Gly71 C^{α} atom) compared with the β-form and the new pocket is

available for TEI-I01800*A* binding. TEI-I01800*A* is twisted around two freely rotatable bonds (C7−N10 and N10−C11) and interacts with this pocket (Figs. 1-6 and 1-7). The methyl group at the 6-position is also important to induce the twisted conformation of the *p*-ethoxyphenylamino group at the 7-position. When the methyl group at the 6-position was removed from TEI-I01800, the inhibitory activity and selectivity clearly decreased (unpublished data). MK2–TEI-I01800 is the first structure to be determined of an α-form MK2 in complex with a small molecule inhibitor and shows that the molecular properties of TEI-I01800*A* cause a secondary structural change of the Gly-rich loop from a β-sheet to an α-helix.

For the binding of TEI-I01800*B*, the *p*-ethoxyphenylamino group at the 7-position of the compound is positioned between the side chains of Tyr260 and Tyr264 (Fig. 1-9).

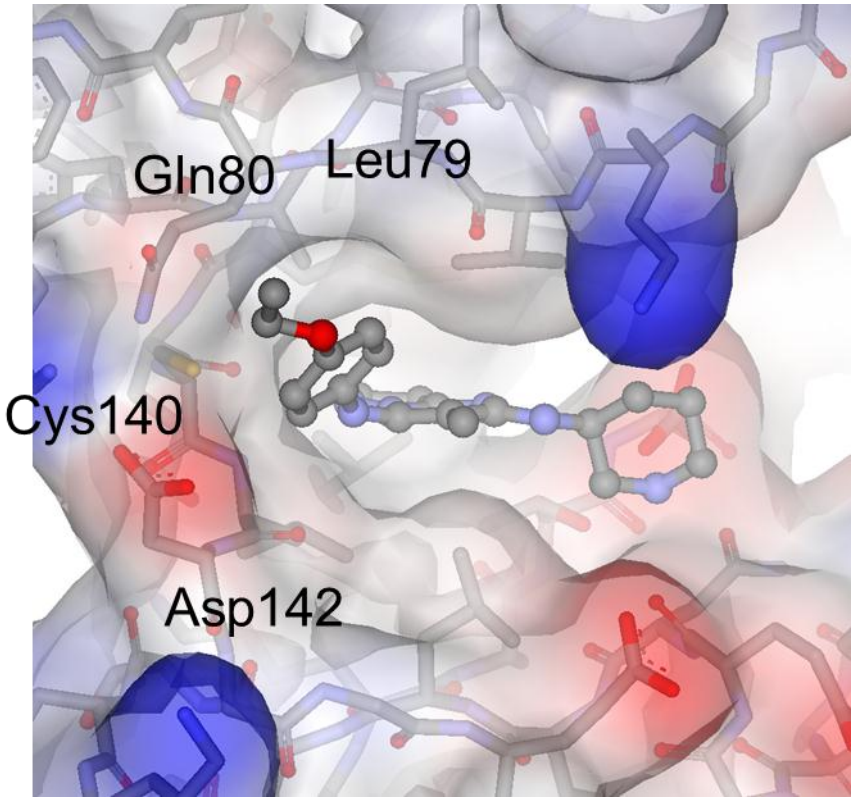

Figure 1-8 Binding interaction of TEII01800*A* and MK2.

Solvent-accessible surface view of the new binding pocket for TEI-I01800*A* (blue shows the electrostatic positive charge and red shows the negative charge as calculated by *DS Visualizer*).

Tyr264 is stacked with the *p*-ethoxyphenyl group by a π–π interaction and there is no hydrogen bond interaction between MK2 and TEI-I01800*B*. The *p*-ethoxyphenyl group at the 7-position of TEI-I01800 might be crucial for the binding of TEI-I01800*B* to the substrate-binding pocket of MK2.

3.2 Structure comparison with apo–MK2 and other MK2–inhibitor complexes

The first crystal structure of MK2 to be determined was the apo form (Meng *et al*., 2002). It is an α-form MK2 in which the auto-inhibitory domain interacts with the substrate-binding pocket. Since its determination, the structures of MK2–AMPPNP, MK2–ADP, MK2–staurosporine and various MK2–small-molecule inhibitor complexes have been reported (Kurumbail *et al*., 2003; Underwood *et al*., 2003; Hillig *et al*., 2007; Anderson *et al*., 2007, 2009; Wu *et al*., 2007). All of these complex structures show a β-form MK2 with a narrow and deep ATP-binding pocket.

In the MK2–TEI-I01800 complex crystal TEI-I01800*B* also binds to MK2 in the substrate-binding pocket. Fig. 1-9 shows a comparison of the substrate-binding pockets in MK2–TEI-I01800*B* and MK2–compound-1 (Hillig *et al*., 2007). TEII01800*B* is sandwiched between a part of the auto-inhibitory domain (molecule *A*, 328–344) and the neighboring molecule (molecule *C*, 229–235) and the substrate-binding pocket is filled by TEI-I01800*B* and these residues (Fig. 1-9*a*). In MK2–compound-1, amino-acid residues 328–350 from molecule *A* and the active segment (amino-acid residues 227–237) from molecule *C* fill this active pocket as shown in Fig. 1-9*b* and therefore it has been proposed that it may represent an intermediate state during substrate phosphorylation (Hillig *et al*., 2007).

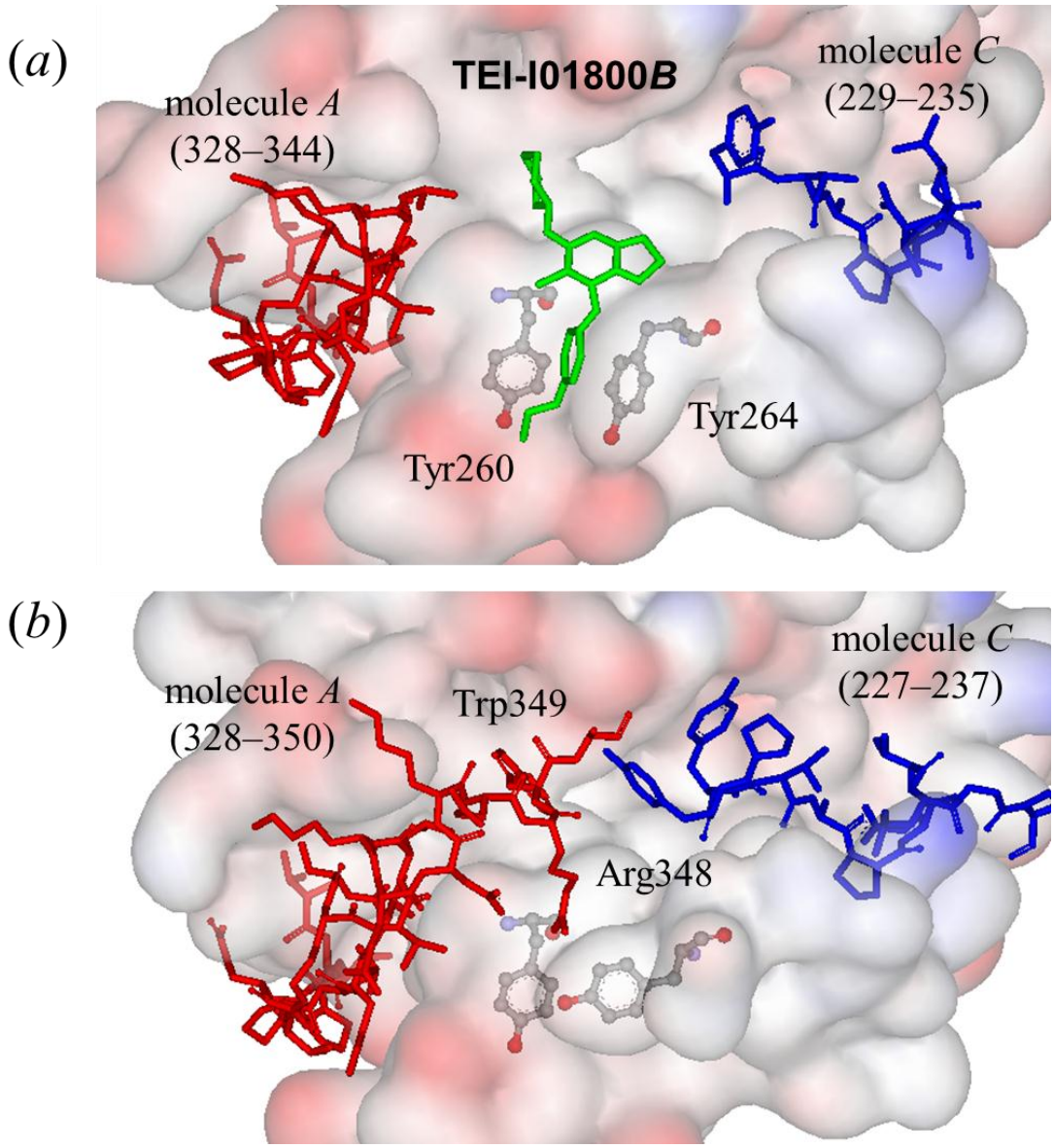

Figure 1-9 Substrate-binding pockets of (*a*) MK2–TEI-I01800*B* and (*b*) MK2–compound-1 (PDB code 2jbp; Hillig *et al*., 2007) viewed from the same angle.

The auto-inhibitory domain residues of Molecule *A*: red and those of neighboring molecule: blue, respectively. TEI-I01800*B* binds between part of the auto-inhibitory domain and residues from the neighboring molecule. The interaction sites of the 5- and 6-positions of TEI-I01800*B* are occupied by Arg348 and Trp349 in the case of MK2–compound-1.

In the MK2–TEI-I01800 complex the density map for residues 345–350 was not visible. In the case of MK2–TEI-I01800 the auto-inhibitory domain may have been pushed out into the solvent area by the binding of TEI-I01800*B*. We also attempted to confirm the binding affinity for TEI-I01800*B* using BIACORE 3000 (GE Healthcare), but the result showed that at least one TEI-I01800 could bind to MK2. In addition, the substrate-competitive bioassay did not show binding of TEI-I01800 in the substrate-binding pocket. Therefore, the binding of the TEI-I01800*B* molecule is considered to be very weak and not suitable for drug discovery.

The Lys93–Glu104 salt bridge is essential in active kinases (Huse & Kuriyan, 2002). Apo–MK2 is in an inactive kinase conformation because the Lys93–Glu104 salt bridge is disrupted and the substrate-binding site is blocked by the auto-inhibitory domain (Fig. 1-10*a*). Apo–MK2 has an α-helical Gly-rich loop. In contrast, MK2–AMP-PNP has a different inactive conformation (with Lys93–Glu104 salt-bridge disruption) that maintains the β-sheet Gly-rich loop (Kurumbail *et al*., 2003). Other MK2–small-molecule complexes (MK2–ADP is shown in Fig. 1-10*c*) apart from MK2–AMP-PNP all show active conformations with a Lys93–Glu104 salt bridge and a β-sheet Gly-rich loop. The β-sheet Gly-rich loop has been considered to be a characteristic feature of active MK2, but the MK2–TEI-I01800 complex is the first active MK2 structure to have a Lys93–Glu104 salt bridge and an α-helical Gly-rich loop (Fig. 1-10*b*).

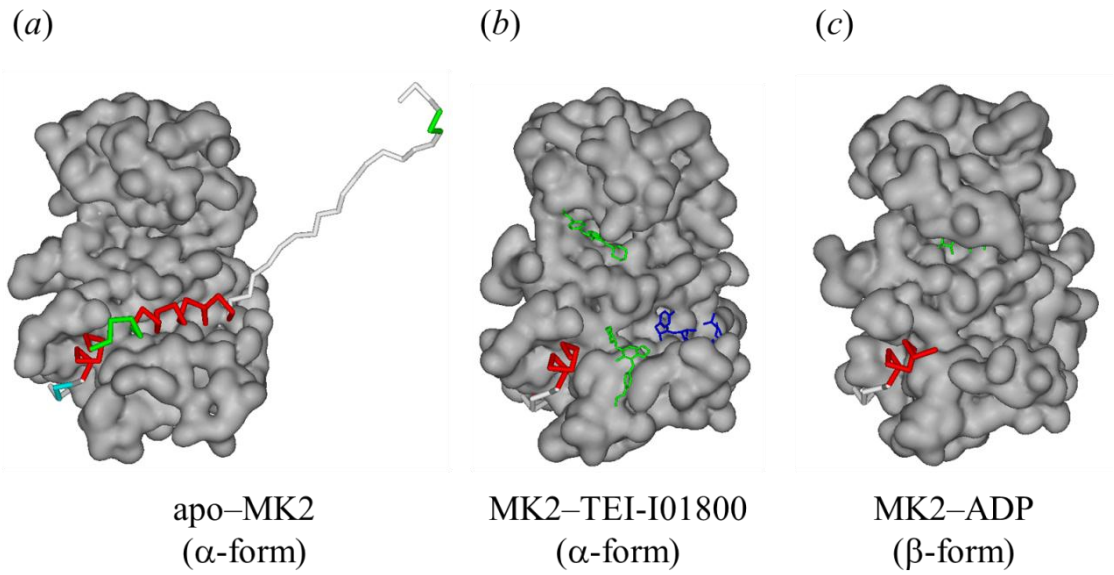

Figure 1- 10 Comparison of surfaces between α-form MK2 and β-form MK2.

The C^{α} wire shows the auto-inhibitory domain (328–400); the inhibitors are shown in green and the residues from the neighboring molecule that form a trimer are shown in blue. (*a*) Apo–MK2 (PDB code 1kwp; Meng *et al*., 2002). The substrate pocket is buried by the auto-inhibitory domain. The Gly-rich loop adopts an α-helical conformation and shows a wide-open ATP-binding pocket. (*b*) MK2–TEI-I01800. TEI-I01800A binds in the wide-open ATP-binding pocket exposed by the α-form Gly-rich loop. TEI-I01800B binds in the substrate-binding pocket. (*c*) MK2–ADP: an active β-form MK2. The ATP molecule binds in the narrow and closed ATP-binding site.

Consequently, we determined the features that cause the structural change of active MK2 from the β-form to the α-form. Fig. 1-11(*a*) shows a superimposed image of MK2–TEI-I01800 onto MK2–compound-1 (the r.m.s.d. on C^{α} atoms between MK2 in the MK2–TEI-I01800 complex and MK2 in the MK2–compound-1 structure is 2.01 Å). The most distinctive difference is in the structure of the Gly-rich loop. Fig. 1-11(*b*) shows that TEI-I01800*A* would collide with the side chain of Leu70 of the Gly-rich loop if MK2 took the β-form (a distance of 1.35 Å between C12/C16 and Leu70 CD1 and an abnormally short distance of 0.83 Å between C13/C15 and Leu70 CD2). On the other hand, Fig. 1-11(*c*) shows a view of the collision

between Leu70 and mercury atom HG5 on superimposing apo–MK2 onto MK2–compound-1 (the r.m.s.d. on C^{α} atoms between these structures is 3.17 Å). The mercury atom of apo–MK2 also might collide with the β-sheet Gly-rich loop (the distance between mercury atom HG5 and Leu70 CD1 is 2.42 Å). In order to avoid those collisions with Leu70, MK2–TEI-I01800 and apo–MK2 adopt an α-helical Gly-rich loop. The TEI-I01800*A* molecule regulates the secondary structure of the Gly-rich loop of MK2.

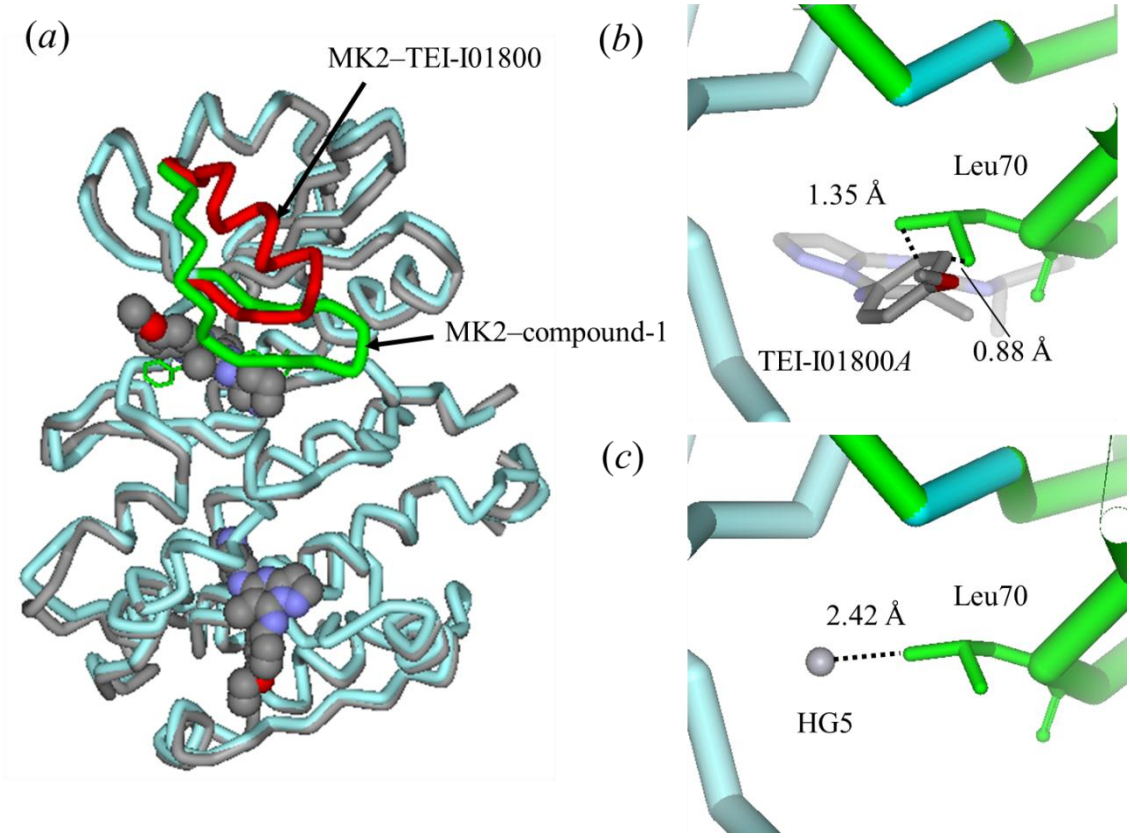

Figure 1-11 Superposition of MK2–TEI-I01800 and apo–MK2 onto β-form MK2.

(*a*) MK2–TEI-I01800 (grey) is superposed onto β-form MK2 (MK2–compound-1, blue). The r.m.s.d. on C^{α} atoms is 2.01 Å. The Gly-rich loop residues 65–80 of MK2–TEI-I01800 are shown in red and those of MK2–compound-1 are shown in green. (*b*) View of the collision between TEI-I01800*A* and Leu70 CD1 of β-form MK2, (*c*) view of the collision between HG5 and Leu70 CD1 of β-form MK2 on superposing Apo–MK2 onto MK2–compound-1. The r.m.s.d. on C^{α} atoms is 3.17 Å.

3.3 TEI-I01800 regulates the secondary structure of the Gly-rich loop

TEI-I01800 has two freely rotatable bonds between the pyrazolo[1,5-*a*] pyrimidine scaffold part and the *p*-ethoxyphenyl group at the 7-position and these bonds result in the structural features of TEI-I01800. Moreover, the methyl group at the 6-position also causes a steric hindrance to the *p*-ethoxyphenylamino group at the 7-position and determines the non-planar conformation of TEI-I01800. As described above, TEI-I01800 can interact with the new binding pocket resulting from the conformational change from a β-sheet to an α-helix, allowing a favorable interaction between the *p*-ethoxyphenylamino group at the 7-position and Cys140 and Leu141. As the other inhibitors in published MK2–inhibitor structures do not contain a twisted functional group near Leu70, they are able to interact with β-form MK2 (Fig. 1-12).

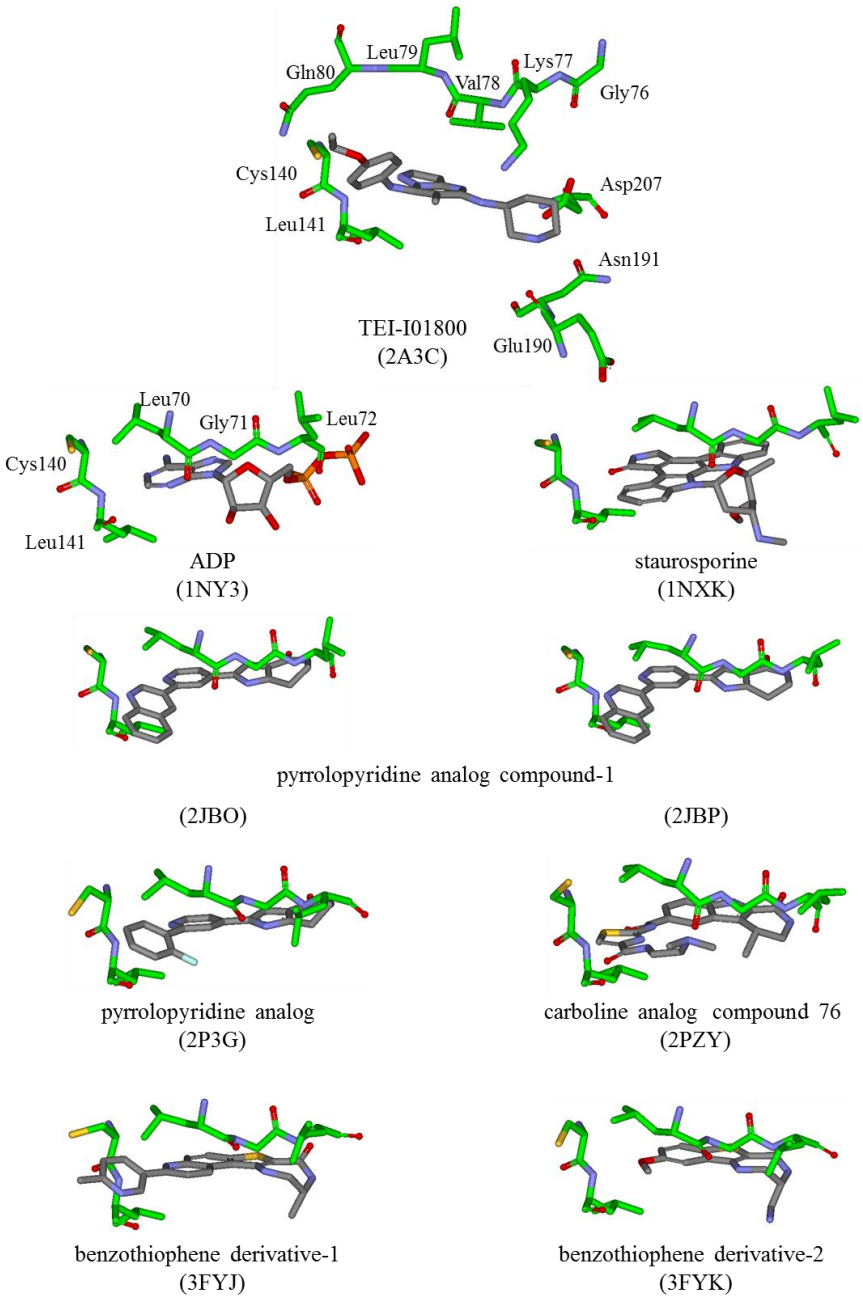

Figure 1-12 Three-dimensional structures of compounds bound to MK2.

The compound names are shown under the structures and PDB codes are shown in parentheses. In MK2–TEI-I01800 (PDB code 2a3c), Leu70–Leu72 and Lys77–Gln80 of the α-helical Gly-rich loop and the residues that interact with TEI-I01800 are shown. In the other complexes, Leu70–Leu72 of the β-sheet Gly-rich loop, Cys140 and Leu141 are shown in green. The directions of these are matched. Only TEI-I01800 regulates the Gly-rich loop and interacts with Cys140 and Leu141.

Therefore, the trigger of the conformational change is TEI-I01800 binding to avoid collide with Leu70 of β-form MK2. Abbott Laboratories have recently reported a new MK2 (47–366, T222E mutant) and its complex with an inhibitor (Argiriadi *et al*., 2009). The atomic coordinates of these structures have not yet been deposited in the PDB; however, the Gly-rich loop of the structure described in this study appears to form an α-helix. It is probable that this inhibitor may also regulate the secondary structure of the Gly-rich loop.

4 Conclusion

We determined the crystal structure of the MK2–TEI-I01800 complex. In the MK2–TEI-I01800 complex structure, we found that the Gly-rich loop adopted an α-helical conformation. TEI-I01800 has a non-planar conformation, unlike other MK2 inhibitors. In order to avoid collision with Leu70, TEI-I01800 causes a secondary structural change of the Gly-rich loop from a β-sheet to an α-helix. The non-planarity of TEI-I01800 allows it to make a stable interaction with the new binding pocket exposed by the α-form MK2. Previously, the presence of β-form MK2 had been considered to be a characteristic feature of an active kinase, as it had been found in all active MK2–small molecule complexes, but the present study shows that the α-helical Gly-rich loop of MK2 represents an active conformation that maintains the Lys93–Glu104 salt bridge. Moreover, the secondary structure of the Gly-rich loop is regulated by the structural features of the inhibitor. TEI-I01800 shows good selectivity for MK2 over other kinases. Recently, the structure of the CDK2–TEI-I01800 complex was determined in our laboratory and its Gly-rich loop was found to adopt a β-sheet structure (Fujino *et al*, unpublished work). The difference in the inhibitory mechanism of TEI-I01800 is expected to make it useful as a new inhibitor with selectivity for MK2. The present study provides important information for the drug design of inhibitors accompanying the structural change of MK2.

References

1. Anderson, D. R., Meyers, M. J., Kurumbail, R. G., Caspers, N., Poda, G. I., Long, S. A., Pierce, B. S., Mahoney, M. W., Mourey, R. J. & Parikh, M. D. (2009). *Bioorg. Med. Chem. Lett.* **19**, 4882–4884.
2. Anderson, D. R., Meyers, M. J., Vernier, W. F., Mahoney, M. W., Kurumbail, R. G., Caspers, N., Poda, G. I., Schindler, J. F., Reitz, D. B. & Mourey, R. J. (2007). *J. Med. Chem.* **50**, 2647–2654.
3. Argiriadi, M. A., Sousa, S., Banach, D., Marcotte, D., Xiang, T., Tomlinson, M. J., Demers, M., Harris, C., Kwak, S., Hardman, J., Pietras, M., Quinn, L., DiMauro, J., Ni, B., Mankovich, J., Borhani, D. W., Talanian, R. V. & Sadhukhan, R. (2009). *BMC Struct. Biol.* **9**, 16.
4. Beyaert, R., Cuenda, A., Vanden Berghe, W., Plaisance, S., Lee, J. C., Haegeman, G., Cohen, P. & Fiers, W. (1996). *EMBO J*. **15**, 1914–1923.
5. Bricogne, G. (1974). *Acta Cryst*. A**30**, 395–405.
6. Collaborative Computational Project, Number 4 (1994). *Acta Cryst.* D**50**, 760–763.
7. Cowtan, K. (1994). *Jnt CCP4/ESF–EACBM Newsl. Protein Crystallogr.* **31**, 34–38.
8. Cuenda, A., Rouse, J., Doza, Y. N., Meier, R., Cohen, P., Gallagher, T. F., Young, P. R. & Lee, J. C. (1995). *FEBS Lett.* **364**, 229–233.
9. Goldberg, D. R., Choi, Y., Cogan, D., Corson, M., DeLeon, R., Gao, A., Gruenbaum, L., Hao, MH., Joseph, D., Kashem, M.A., Miller, C., Moss, N., Netherton, M. R., Pargellis, C. P., Pelletier, J., Sellati, R., Skow, D., Torcellini, C., Tseng, Y. C., Wang, J., Wasti, R., Werneburg, B., Wu, J.P. & Xiong, Z. (2008). *Bioorg. Med. Chem. Lett.* **18**, 938–941.
10. Gruenbaum, L. M., Schwartz, R.,Woska, J. R. Jr, DeLeon, R. P., Peet, G. W., Warren, T. C., Capolino, A., Mara, L., Morelock, M. M., Shrutkowski, A., Jones, J. W. & Pargellis, C. A. (2009). *Biochem. Pharmacol.* **77**, 422–432.
11. Hillig, R. C., Eberspaecher, U., Monteclaro, F., Huber, M., Nguyen, D., Mengel, A., Muller-Tiemann, B. & Egner, U. (2007). *J. Mol. Biol.* **369**, 735–745.

12. Huse, M. & Kuriyan, J. (2002). *Cell*, **109**, 275–282.
13. Kotlyarov, A., Neininger, A., Schubert, C., Eckert, R., Birchmeier, C., Volk, H. D. & Gaestel, M. (1999). *Nature Cell Biol.* **1**, 94–97.
14. Kurumbail, R. G., Pawlitz, J. L., Stegeman, R. A., Stallings, W. C., Shieh, H.-S., Mourey, R. J., Bolten, S. L. & Brouadus, R. M. (2003). Patent WO/2003/076333.
15. Lee, J. C., Laydon, J. T., McDonnell, P. C., Gallagher, T.F., Kumar, S., Green, D., McNulty, D., Blumenthal, M. J., Heys, J. R., Landvatter S. W., Strickler, J. E., McLaughlin, M. M., Siemens, I. R., Fisher, S.M., Livi, G. P., White, J. R., Adams, J. L. & Young, P. R. (1994). *Nature (London)*, **372**, 739–746.
16. Meng,W., Swenson, L. L., Fitzgibbon, M. J., Hayakawa, K., Ter Haar, E., Behrens, A. E., Fulghum, J. R. & Lippke, J. A. (2002). *J. Biol. Chem*. **277**, 37401–37405.
17. Murshudov, G. N., Vagin, A. A. & Dodson, E. J. (1997). *Acta Cryst.* D**53**, 240–255.
18. Otwinowski, Z. & Minor,W. (1997). *Methods Enzymol*. **276**, 307–326.
19. Pargellis, C., Tong, L., Churchill, L., Cirillo, P. F., Gilmore, T., Graham, A. G., Grob, P. M., Hickey, E. R., Moss, N., Pav, S. & Regan, J. (2002). *Nature Struct. Biol*. **9**, 268–272.
20. Schuller, D. J. (1996). *Acta Cryst.* D**52**, 425–434.
21. Underwood, K. W., Parris, K. D., Federico, E., Mosyak, L., Czerwinski, R. M., Shane, T., Taylor, M., Svenson, K., Liu, Y., Hsiao, C. L., Wolfrom, S., Maguire, M., Malakian, K., Telliez, J. B., Lin, L. L., Kriz, R. W., Seehral, J., Somers, W. S. & Stahl, M. L. (2003). *Structure*, **11**, 627–636.
22. Vagin, A. & Teplyakov, A. (1997). *J. Appl. Cryst*. **30**, 1022–1025.
23. Wu, J. P., Wang, J., Abeywardane, A., Andersen, D., Emmanuel, M., Gautschi, E., Goldberg, D. R., Kashem, M. A., Lukas, S., Mao, W., Martin, L., Morwick, T., Moss, N., Pargellis, C., Patel, U. R., Patnaude, L., Peet, G. W., Skow, D., Snow, R. J., Ward, Y., Werneburg, B. & White, A. (2007). *Bioorg. Med. Chem. Lett*. **17**, 4664–4669.
24. Xiong, Z., Gao, D. A., Cogan, D. A., Goldberg, D. R., Hao, M. H., Moss, N., Pack, E., Pargellis, C., Skow, D., Trieselmann, T., Werneburg, B. & White, A. (2008). *Bioorg. Med. Chem. Lett.* **18**, 1994–1999.

25. Yao, M., Zhou, Y. & Tanaka, I. (2006). *Acta Cryst.* D**62**, 189–196.

26. Zhou, Y., Yao, M. & Tanaka, I. (2006). *J. Appl. Cryst*. **39**, 57–63.

Chapter 2

Crystal structure of human cyclin-dependent kinase-2 complex with MK2 inhibitor TEI-I01800: insight into the selectivity

Summary

Mitogen-activated protein kinase-activated protein kinase 2 (MK2 or MAPKAP-K2) is a Ser/Thr kinase from the p38 mitogen-activated protein kinase signaling pathway and plays an important role in inflammatory diseases. The crystal structure of the MK2–TEI-I01800 complex has been reported; its Gly-rich loop was found to form an α-helix, not a β-sheet as has been observed for other Ser/Thr kinases. TEI-I01800 is 177-fold selective for MK2 compared with CDK2; in order to understand the inhibitory mechanism of TEII01800, the cyclin-dependent kinase 2 (CDK2) complex structure with TEI-I01800 was determined at 2.0 Å resolution. Interestingly, the Gly-rich loop of CDK2 formed a β-sheet that was different from that of MK2. In MK2, TEI-I01800 changed the secondary structure of the Gly-rich loop from a β-sheet to an α-helix by collision between Leu70 and a *p*-ethoxyphenyl group at the 7-position and bound to MK2. However, for CDK2, TEI-I01800 bound to CDK2 without this structural change and lost the interaction with the substituent at the 7-position. In summary, the results of this study suggest that the reason for the selectivity of TEI-I01800 is the favorable conformation of TEI-I01800 itself, making it suitable for binding to the α-form MK2.

1 Introduction

Mitogen-activated protein kinase-activated protein kinase 2 (MK2 or MAPKAP-K2) is one of the Ser/Thr kinases from the p38 mitogen activated protein kinase signaling pathway, which has been shown to play an important role in the production of TNF-α and other cytokines (Beyaert *et al*., 1996). TNF-α is implicated in several inflammatory diseases such as rheumatoid arthritis, and therefore inhibition of TNF-α activity represents a most promising target for anti-inflammatory therapy (Camussi & Lupia, 1998; Kotlyarov *et al*., 1999). Several groups have reported programs to develop anti-inflammatory therapies through the generation of MK2 inhibitors and determined the crystal structure of MK2 (Wu *et al*., 2007; Hillig *et al*., 2007; Velcicky *et al*., 2010; Anderson *et al*., 2007, 2009*a*,*b*; Revesz *et al*., 2010; Argiriadi *et al*., 2009, 2010; Fujino *et al*., 2010; Barf *et al*., 2011). With the exception of two inhibitor complex structures, TEI-I01800 [the RCSB Protein Data Bank (PDB) code 3a2c; Fujino *et al*., 2010] and 2,4-diaminopyrimidine derivative from Abott (PDB code 3ka0; Argiriadi *et al*., 2010), all MK2 complexes deposited in the PDB have a β-sheet Gly-rich loop (β-form). In a previous study (Fujino *et al*., 2010) we revealed that the MK2 complex with TEI-I01800 has a unique α-helical Gly-rich loop (α-form) and TEI-I01800 binds to a specific hydrophobic pocket exposed by the structural change.

Protein kinases are key regulators of cell function that constitute one of the largest and most functionally diverse gene families. Kinases are particularly prominent in signal transduction and coordination of complex functions. In particular, cyclin-dependent kinase 2 (CDK2), which is also a member of the Ser/Thr kinase family, plays a central role in the control of the cell cycle (Tsai *et al*., 1991), so interference with the cell cycle via inhibition is likely to be an undesirable feature for anti-inflammatory drugs used chronically such as MK2 inhibitor; in fact, the improvement of selectivity over CDK2 has been published (Anderson *et al*., 2009*a*, *b*; Kosugi *et al*., 2012). MK2 and CDK2 complex structures with the same inhibitor which has only 29-fold selectivity for MK2 are reported and the interaction mode is observed to look similar (Anderson *et al*., 2009*a*). These structures show that it is difficult to obtain selectivity for MK2 by

interaction with the hinge region.

TEI-I01800 shows a good potency and selectivity for significant kinases and has 177-fold selectivity for MK2 over CDK2. In this study we present a CDK2–TEI-I01800 complex structure for the purpose of better understanding of the binding mode and the structure guided drug design. Consequently, the Gly-rich loop of CDK2 keeps the β-form and TEI-I01800 binds to CDK2 with an unfavorable conformation compared with the stable conformer TEI-I01800 itself. The results indicate that TEI-I01800 is a specific compound which causes the structural change of the Gly-rich loop of MK2, not CDK2, to increase selectivity for MK2.

2 Materials and methods

Inactive monomeric human CDK2 was expressed in Tn5 insect cells using a recombinant baculovirus encoding CDK2 gene and purified as described in the literature with slight modification (Rosenblatt *et al*., 1993). The purified CDK2 was concentrated to 5–10 mg ml^{-1} and crystallization experiments of apo–CDK2 were performed using the sitting-drop vapor diffusion method under the conditions of 0.1 *M* HEPES pH 7.4, 10–15% PEG 3350 and 50 m*M* ammonium acetate. After the crystals were grown for 2–3 days, TEI-I01800, which was synthesized by Kosugi *et al*. (2012), was added to the crystallization drop at a final concentration of 2 m*M* and soaked for 12–24 hours. X-ray diffraction data were collected on beamline BL32B2 at SPring-8 at 100 K using 25% glycerol as cryoprotectant. The CDK2–TEI-I01800 complex crystals diffracted to 2.0 Å resolution and belonged to space group $P2_12_12_1$ with unit-cell parameters a = 53.64, b = 72.10 and c = 72.61 Å. The reflection data were processed using *CrystalClear* 1.3.5 (Rigaku) and molecular replacement was carried out using *MOLREP* (Vagin & Teplyakov, 1997) from CCP4 (Collaborative Computational Project, 1994) with the CDK2 structure (PDB code 1fvt) without ligand and waters as the initial model. Structure refinement was carried out using the program *REFMAC* (Murshudov *et al*., 1997). After rigid-body refinement, the electron density for TEI-I01800 was clearly found and assigned using *COOT* (Emsley & Cowtan, 2004). The structure refinement was continued until the R and R_{free} factors were 18.9% and 24.9%, respectively. Statistics of the data collection and final structure are summarized in Table 2-1. Methods for measurement of MK2 and CDK2 enzyme assay were described in our previous paper (Kosugi *et al*., 2012). Structure minimization of the protein–ligand complex with OPLS 2005 force field was performed using the *Protein Preparation Wizard*. Conformational search and potential energy calculation was carried out using *Macromodel* in the Schrödinger software suite (http://www.schrodinger.com/). All figures were produced using *Discovery Studio* (Accelrys Inc.; http://accelrys.com/).

	CDK2–TEI-I01800
Data collection	
Beamline	SPring-8 BL32B2
Wavelength (Å)	1.000
Resolution (Å)	50.00-2.00 (2.07-2.00)
Mosaicity (°)	0.30
No. of unique reflections	19590
R_{merge} (%)	5.9 (20.4)
Completeness (%)	99.9 (100.0)
Multiplicity	7.03 (7.23)
Average $I/\sigma(I)$	18.5 (8.4)
Space group	$P2_12_12_1$
Unit-cell parameters (Å)	
a	53.64
b	72.10
c	72.61
Refinement	
Resolution (Å)	20.0-2.0
R factor (%)	18.9
R_{free} (%)	24.9
No. of reflections (work/test)	18564/1001
R.m.s.d. from ideal values	
Bond lengths (Å)	0.018
Bond angles (°)	1.64

Table 2-1 Data-collection and refinement statistics.

Values in parentheses are for the highest resolution shell.

3 Results and discussion

3.1 Overall structure of CDK2–TEI-I01800 and the binding mode of TEI-I01800

The overall structure of the CDK2–TEI-I01800 complex is very similar to that of other CDK2 structures. The density maps from Val154 to Glu162 (T-loop) are disordered. In spite of its weak inhibition, the electron density map of TEI-I01800 is clearly found in the ATP-binding pocket at the N-terminal domain, and TEI-I01800 binds to CDK2 with several hydrogen bond interactions (Figs. 2-1 and 2-2).

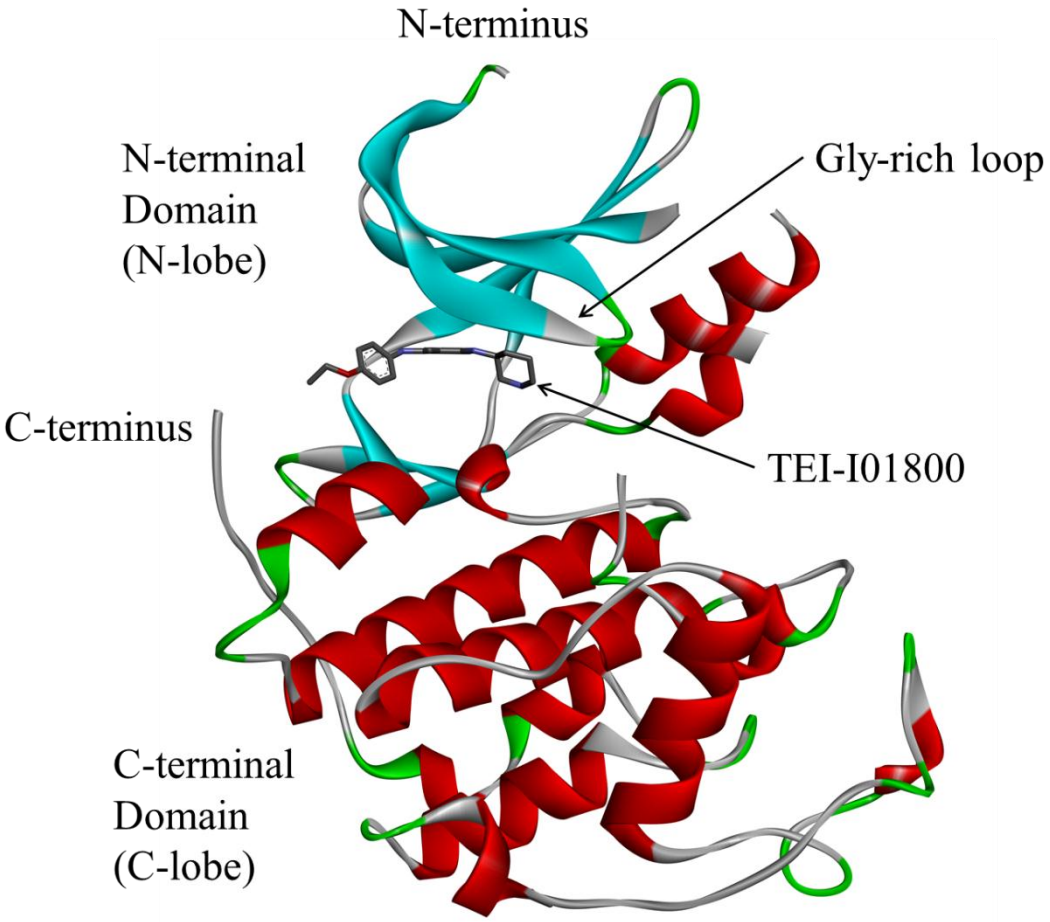

Figure 2-1 Overall structure of the CDK2–TEI-I01800 complex.

The overall kinase fold of CDK2 is shown in ribbon representation (α-helices are shown in red, β-sheets in blue and β-turns in green). TEI-I01800 bound to CDK2 in the ATP-binding site.

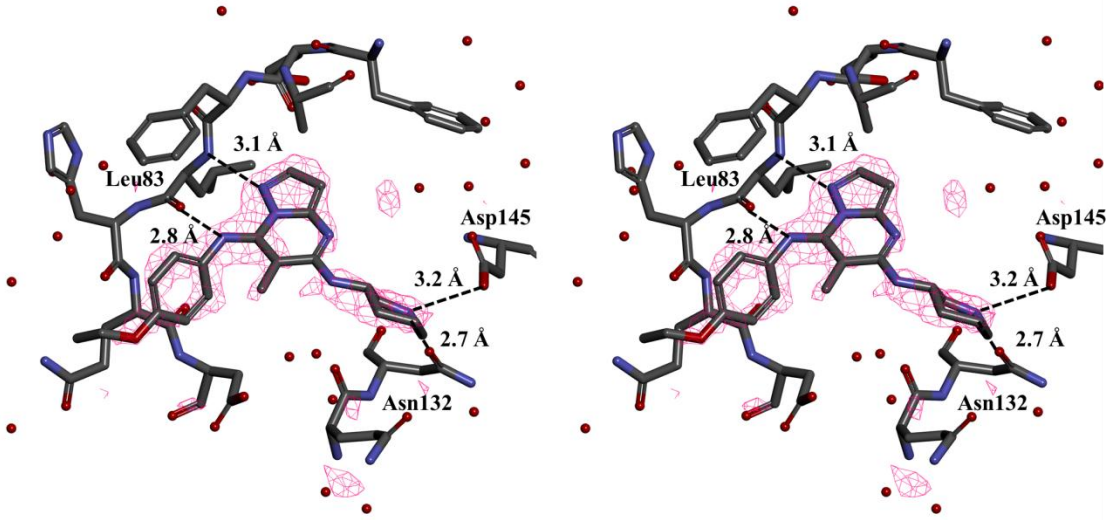

Figure 2-2 Stereo diagram of the electron density map of TEI-I01800 and interactions.

The electron density map of TEI-I01800 is drawn by $F_o - F_c$ OMIT map contoured at 3.0 σ.

The molecular structure and atomic numbering of TEI-I01800 are shown in Fig. 2-3. It has a pyrazolo[1,5-*a*]pyrimidine scaffold with a (3*S*)-piperidylamino group at the 5-position, a methyl group at the 6-position and a *p*-ethoxyphenylamino group at the 7-position. Its inhibitory activities (IC_{50} values) for CDK2 and for MK2 are 23 and 0.13 μ*M*, respectively.

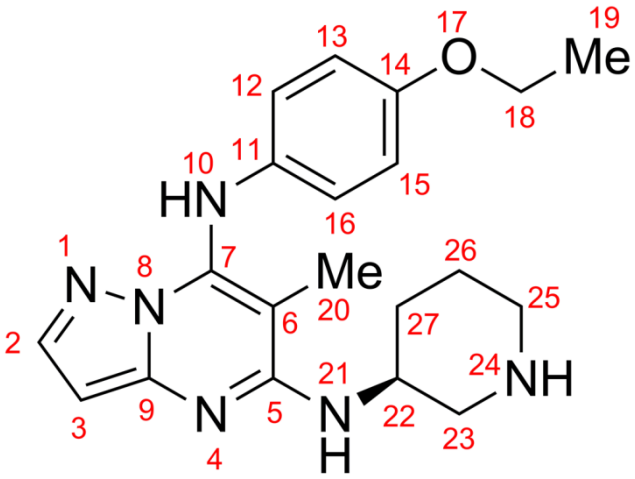

Figure 2-3 Schematic molecular structure of TEI-I01800.

Atom numbers were assigned sequentially. The bonds C7−N10 and N10−C11 between the pyrazolo[1,5-*a*]pyrimidine-scaffold part and the *p*-ethoxyphenyl group at the 7-position are freely rotatable.

As shown in Fig. 2-2, TEI-I01800 interacts with the backbone amide of Leu83 and through two hydrogen bonds: TEII01800 N1—Leu83 N (3.1 Å) and TEI-I01800 N10—Leu83 O (2.8 Å). The N24 atom of TEI-I01800 might be ionized and make a hydrogen bond to the carboxyl group of Asp145 (3.2 Å). This atom also makes one additional hydrogen bond to the OD1 atom of Asn132 (2.7 Å). TEI-I01800 is twisted around two freely rotatable bonds (C7–N10 and N10–C11) and the *p*-ethoxyphenylamino group at the 7-position is slightly twisted toward the C-terminal domain to avoid steric hindrance.

3.2 Structure comparison with other CDK2 structures

At present, 335 structures of human CDK2 are available from the PDB, 237 of them are inactive monomeric CDK2, and almost all are complexes with small inhibitors for drug design. The others are active heteromers with several kinds of cyclin molecules; they show the large conformational change of the ^{45}PSTAIRE^{51} helix, the T-loop and the Gly-rich loop (Jeffrey *et al*., 1995). In our study the inactive CDK2 was selected to develop the selective MK2 inhibitor, because the SAR (structure activity relationship) for this series is correlated with X-ray structure

analysis.

The Gly-rich loop of CDK2 is considered flexible because it moves by the binding of the inhibitor or cyclin. However, all CDK2 with the exception of CDK2/cyclinA/peptide inhibitor p27KipK (Russo *et al*., 1996) keep the β-form and the secondary structural change as of MK2–TEI-I01800 is not found. This suggests that the β-form is stable in CDK2–small inhibitor complexes and the structural change to the α-form does not occur. Figure 2-4 shows the superimposition of CDK2–TEI-I01800 on the highest resolution apo–CDK2 (PDB code 4ek3; Kang & Stuckey, 2013) and a pyrazolo[1,5-*a*]pyrimidine inhibitor which has the same scaffold as TEI-I01800 from the Vernalis complex (PDB code 1y91; Williamson *et al*., 2005).

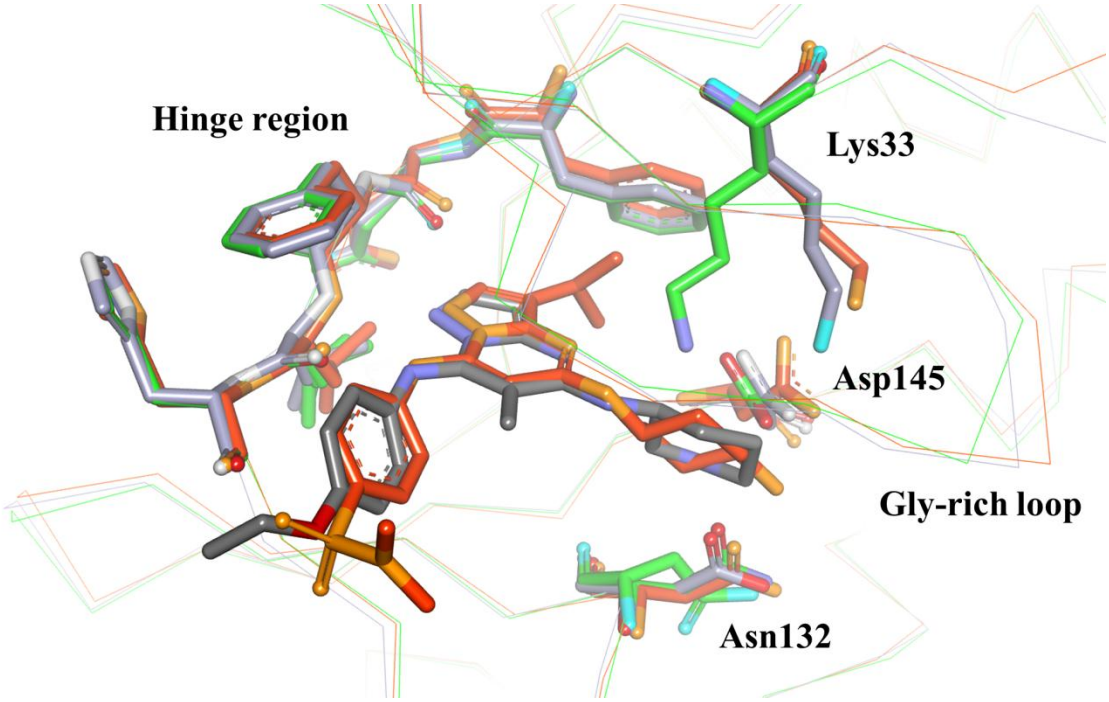

Figure 2-4 Comparison of binding interactions between apo–CDK2 and CDK2–inhibitors.

Superposing of the CDK2–TEI-I01800 (grey) on the apo–CDK2 (green) and the CDK2–pyrazolo[1,5-*a*]pyrimidine inhibitor from Vernalis (orange).

The root-mean-square deviations (r.m.s.d.) between C^{α} atoms are 0.83 and 0.55 Å, respectively. Although the overall structure is almost the same including the Gly-rich loop structure, there are two differences found between apo–CDK2 and complexes. One is Lys33 and Asp145, and the other is the lack of part of a T-loop. In apo–CDK2, Lys33 makes a salt bridge with Asp145, but, in complex, Asp145 contacts with the ligand amine, and Lys33–Asp145 bonding is broken. As described in the literature (Wu *et al*., 2003), the movement of Lys33, Asp145 and adjacent Tyr15 results in an induced movement of the Gly-rich loop and rearrangement adjacent to the T-loop. The disorder of the T-loop found in CDK2–inhibitor may be caused by the movement of Lys33 and Asp145. The binding conformation and interaction of the CDK2–Vernalis compound is very similar to that of TEI-I01800, except for the interaction between Phe80 and an isopropyl moiety at the 3-position. Because our study also showed that this area is a promising region for CDK2 activity, we focused on positions other than the 3-position. Although we expected the dihedral angle between the pyrazolopyrimidine scaffold and the 7-position moiety of TEI-I01800 to be large based on the result of the MK2–TEI-I01800 analysis, no significant difference was shown in comparison with the Vernalis compound which is unsubstituted at the 6-position.

3.3 Conformational analysis of TEI-I01800

As described in our previous paper (Kosugi *et al*., 2012), the selectivity of TEI-I01800 derivatives was increased by methylation at the 6-position. In order to understand the effect of the methyl group at the 6-position, conformational analyses were performed. The ideal dihedral angle of TEI-I01800 between the 7-position substituent and the pyrazolo[1,5-*a*]pyrimidine scaffold (C6–C7–N10–C11) is calculated to be 58.4º because the 7-p-ethoxyphenyl group and the 6-methyl group are twisted by the steric hindrance. When the 6-methyl group is removed, the calculated dihedral angle decreases to 18.8º and the position of the 7-*p*-ethoxyphenyl group is clearly different as shown in Fig. 5. This analysis strongly supports our SAR data that the non-planar conformation of TEI-I01800 is important for MK2 inhibition. On the other hand, the observed dihedral angle of TEI-I01800 binding to CDK2 is smaller (−29.2º) than that of MK2

(44.9º), which is measured after structural idealization by the energy minimization, and the potential energies are calculated as −120.7 kcal mol $^{-1}$and −309.8 kcal mol^{-1}, respectively. The result indicates that the planar conformation of TEI-I01800 as found in CDK2 is unstable compared with the non-planar conformation of TEII01800 found in the MK2 complex.

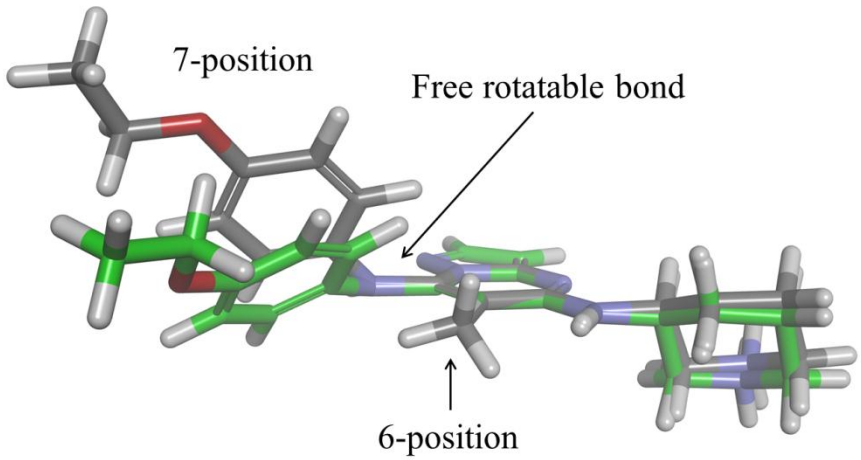

Figure 2-5 Comparison of ideal stable conformers of TEI-I01800 and TEI-I01800 without the methyl group at the 6-position.

Stable conformer of TEI-I01800 is shown in grey and TEI-I01800 without the methyl group at the 6-position is shown in green. The ideal dihedral angle of TEI-I01800 between the scaffold and the substitution of at the 7-position is larger than that of TEI-I01800 lacking of the methyl group at the 6-position.

3.4 Structure comparison with MK2–TEI-I01800 and selectivity of TEI-I01800

CDK2 was superimposed on MK2 by the least-squares method between main-chain atoms against the residues Phe80–Leu83 (Met138–Leu141 in MK2), Asn132 and Asp145 (Asn191 and Asp207 in MK2); the r.m.s.d. value calculated for these six residues is 0.80 Å and that for 180 residues which are aligned by a superimposed structure is 2.93 Å. The ATP-binding sites with the exception of the Gly-rich loop are well overlapped. The two hydrogen bond interactions, as

in MK2, between the hinge region and TEI-I01800 are slightly stronger than that of the MK2–TEI-I01800 complex (TEI-I01800 N1—Leu141 N is 3.1 Å and TEI-I01800 N10—Leu141 O is 3.3 Å); this result is consistent with other reports (Anderson *et al*., 2009*a*). However, the number of hydrogen bonds between CDK2 and the 5-(3*S*)-piperidylamino group is less than for MK2 which has an additional hydrogen bond (TEI-I01800 N10—Glu190 O; 2.8 Å). The lacking of hydrogen bond is one factor of the selectivity, but our result indicates a more interesting mechanism.

The ATP-binding pockets of MK2 and CDK2 with TEII01800 are shown in Fig. 2-6.

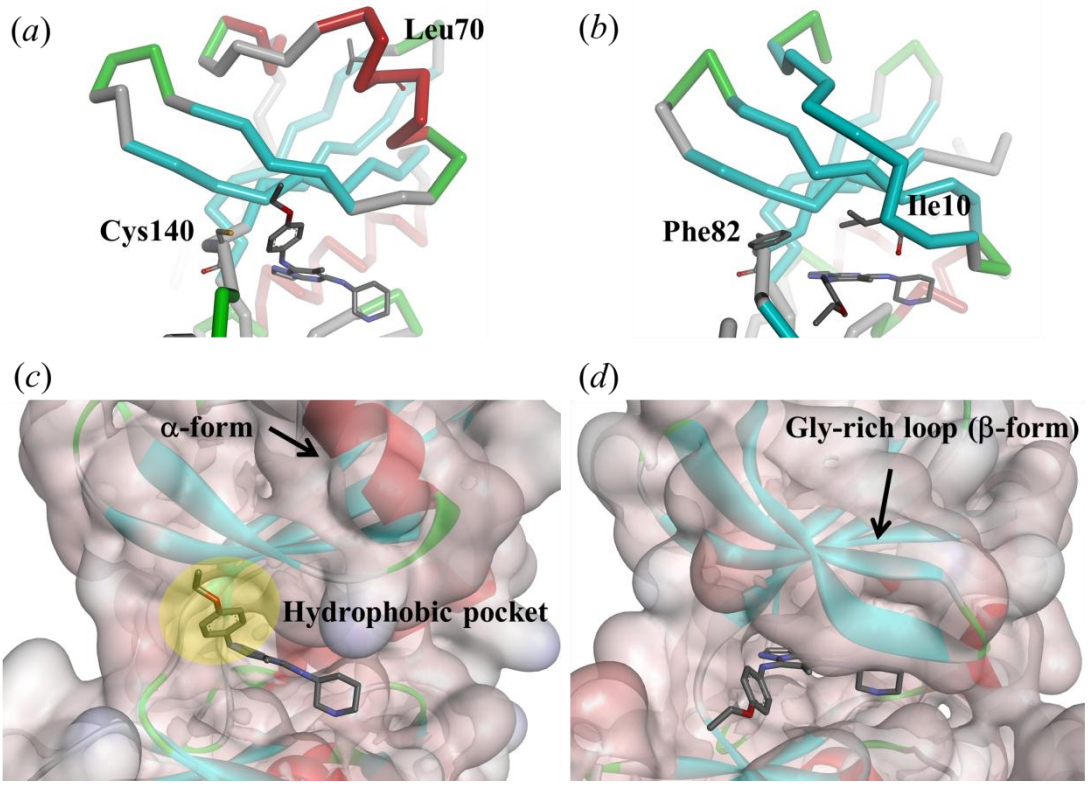

Figure 2-6 ATP-binding pocket of (*a*), (*c*) MK2 and (*b*), (*d*) CDK2 bound to TEII01800.

The key residues of structural change Cys140, Leu70 (MK2), Phe82 and Ile10 (CDK2) are drawn by stick representation.

In MK2–TEI-I0800 the Gly-rich loop flips up toward the N-terminal domain by collision between Leu70 and TEI-I01800 and forms the α-helical Gly-rich loop. Then, this structural change induces the hydrophobic pocket for the binding of the *p*-ethoxyphenyl group at the 7-position. Because the optimization of the 7-position clearly showed an improvement in the MK2 activity, the interaction between this pocket and TEI-I01800 is considered important (Kosugi *et al*., 2012). On the other hand, CDK2 cannot be induced to an α-form by TEI-I01800 although Ile10 which corresponds to Leu70 in MK2 has the possibility to be a trigger of such a structural change. Two reasons why CDK2 does not undergo the structural change as MK2 are considered. One is that the β-form of CDK2 is more stable than the α-form compared with MK2 because, although a huge number of monomeric inactive CDK2 complex structures with various inhibitors have been reported in the PDB, there is no α-form CDK2. The other reason is that Phe82 in CDK2 is larger than Cys140 in MK2 and could cause a second collision between Phe82 and a stable conformer of TEI-I01800 binding to MK2 (CE1—C17 is 1.9 Å and CE1—C20 is 2.0 Å). As a result, CDK2 cannot take the α-form, and the binding pocket, which is not favorable for binding with the stable conformer of TEII01800, has a distinct shape compared with that of MK2.

As described above, because the stable conformer of TEII01800 matches the binding conformation of TEI-I01800 in MK2, TEI-I01800 can stably bind to MK2, which has the possibility of causing a structural change of the Gly-rich loop. However, when TEI-I01800 binds to the β-form of CDK2, the dihedral angle between the 7-position substituent and the scaffold must be arranged in an unfavorable conformation. In conclusion, the results indicate that the characteristic α-form structure of MK2 suitable for TEI-I01800 binding and the favorable interaction different from that of CDK2 is the main reason for the selectivity of TEI-I01800.

4 Conclusion

In this research we present the CDK2 structure bound to potent and selective MK2 inhibitor TEI-I01800. Although TEI-I01800 creates the α-form MK2 by collision with Leu70, in CDK2 TEI-I01800 does not change the Gly-rich loop structure. Instead, the conformation of TEI-I01800 itself is arranged so that it is possible to interact with the β-form CDK2. TEI-I01800, which is a non-planar structure due to the steric hindrance between the 6-methyl group and the 7-pethoxyphenyl group, cannot keep the stable non-planar conformation in the narrow ATP-binding pocket in the β-form CDK2. Thus, it binds with an unstable conformation and also lacks the important interaction with the *p*-ethoxyphenyl substituent at the 7-position for MK2 inhibitory activity. We conclude that this difference is the reason TEI-I01800 demonstrates the selectivity for MK2 and not CDK2.

In the development of kinase inhibitors, since the shape of the ATP-binding pocket is quite similar, it is very difficult to have selectivity for antitarget kinases. As this study has shown, the selective inhibitor can change the protein structure to arrange the shape of the pocket suitable for binding by the compound itself. The mechanism of such an induced-fit means that it will become possible to acquire a compound with higher selectivity.

References

1. Anderson, D. R., Meyers, M. J., Kurumbail, R. G., Caspers, N., Poda, G. I., Long, S. A., Pierce, B. S., Mahoney, M. W. & Mourey, R. J. (2009*a*). *Bioorg. Med. Chem. Lett*., **19**, 4878–4881.
2. Anderson, D. R., Meyers, M. J., Kurumbail, R. G., Caspers, N., Poda, G. I., Long, S. A., Pierce, B. S., Mahoney, M. W., Mourey, R. J. & Parikh, M. D. (2009*b*). *Bioorg. Med. Chem. Lett*. **19**, 4882–4884.
3. Anderson, D. R., Meyers, M. J., Vernier, W. F., Mahoney, M. W., Kurumbail, R. G., Caspers, N., Poda, G. I., Schindler, J. F., Reitz, D. B. & Mourey, R. J. (2007). *J. Med. Chem*. **50**, 2647–2654.
4. Argiriadi, M. A., Ericsson, A. M., Harris, C. M., Banach, D. L., Borhani, D. W., Calderwood, D. J., Demers, M. D., Dimauro, J., Dixon, R. W., Hardman, J., Kwak, S., Li, B., Mankovich, J. A., Marcotte, D., Mullen, K. D., Ni, B., Pietras, M., Sadhukhan, R., Sousa, S., Tomlinson, M. J., Wang, L., Xiang, T. & Talanian, R. V. (2010). *Bioorg. Med. Chem. Lett*. **20**, 330–333.
5. Argiriadi, M. A., Sousa, S., Banach, Marcotte, Xiang, Tomlinson, M. J., Demers, Harris, Kwak, S., Hardman, J., Pietras, M., Quinn, L., DiMauro, J., Ni, B., Mankovich, Borhani, W., Talanian, R. V. & Sadhukhan, R. (2009). *BMC Struct. Biol*. **9**, 16.
6. Barf, T., Kaptein, A., de Wilde, S., van der Heijden, R., van Someren, R., Demont, D., Schultz-Fademrecht, C., Versteegh, J., van Zeeland, M., Seegers, N., Kazemier, B., van de Kar, B., van Hoek, M., de Roos, J., Klop, H., Smeets, R., Hofstra, C., Hornberg, J. & Oubrie, A. (2011). *Bioorg. Med. Chem. Lett*. **21**, 3818–3822.
7. Beyaert, R., Cuenda, A., Vanden Berghe, W., Plaisance, S., Lee, J. C., Haegeman, G., Cohen, P. & Fiers, W. (1996). *EMBO J*. **15**, 1914–1923.
8. Camussi, G. & Lupia, E. (1998). *Drugs*, **55**, 613–620.
9. Collaborative Computational Project, Number 4 (1994). *Acta Cryst*. D**50**, 760–763.
10. Emsley, P. & Cowtan, K. (2004). *Acta Cryst.* D**60**, 2126–2132.

11. Fujino, A., Fukushima, K., Namiki, N., Kosugi, T. & Takimoto- Kamimura, M. (2010). *Acta Cryst.* D**66**, 80–87.
12. Hillig, R. C., Eberspaecher, U., Monteclaro, F., Huber, M., Nguyen, D., Mengel, A., Muller-Tiemann, B. & Egner, U. (2007). *J. Mol. Biol*. **369**, 735–745.
13. Jeffrey, P. D., Russo, A. A., Polyak, K., Gibbs, E., Hurwitz, J., Massagué, J. & Pavletich, N. P. (1995). *Nature (London)*, **376**, 313–320.
14. Kang, Y. N. & Stuckey, J. A. (2013). To be published.
15. Kosugi, T., Mitchell, D. R., Fujino, A., Imai, M., Kambe, M., Kobayashi, S., Makino, H., Matsueda, Y., Oue, Y., Komatsu, K., Imaizumi, K., Sakai, Y., Sugiura, S., Takenouchi, O., Unoki, G., Yamakoshi, Y., Cunliffe, V., Frearson, J., Gordon, R., Harris, C. J., Kalloo-Hosein, H., Le, J., Patel, G., Simpson, D. J., Sherborne, B., Thomas, P. S., Suzuki, N., Takimoto-Kamimura, M. & Kataoka, K. (2012). *J. Med. Chem*. **55**, 6700–6715.
16. Kotlyarov, A., Neininger, A., Schubert, C., Eckert, R., Birchmeier, C., Volk, H. D. & Gaestel, M. (1999). *Nat. Cell Biol*. **1**, 94–97.
17. Murshudov, G. N., Vagin, A. A. & Dodson, E. J. (1997). *Acta Cryst*. D**53**, 240–255.
18. Revesz, L., Schlapbach, A., Aichholz, R., Dawson, J., Feifel, R., Hawtin, S., Littlewood-Evans, A., Koch, G., Kroemer, M., Möbitz, H., Scheufler, C., Velcicky, J. & Huppertz, C. (2010). *Bioorg. Med. Chem. Lett*. **20**, 4719–4723.
19. Rosenblatt, J., De Bondt, H., Jancarik, J., Morgan, D. O. & Kim, S. H. (1993). *J. Mol. Biol*. **230**, 1317–1319.
20. Russo, A. A., Jeffrey, P. D., Patten, A. K., Massagué, J. & Pavletich, N. P. (1996). *Nature (London)*, **382**, 325–331.
21. Tsai, L. H., Harlow, E. & Meyerson, M. (1991). *Nature*, **353**, 174–177.
22. Vagin, A. & Teplyakov, A. (1997). *J. Appl. Cryst*. **30**, 1022–1025.
23. Velcicky, J., Feifel, R., Hawtin, S., Heng, R., Huppertz, C., Koch, G., Kroemer, M., Moebitz, H., Revesz, L., Scheufler, C. & Schlapbach, A. (2010). *Bioorg. Med. Chem. Lett*. **20**, 1293–1297.
24. Williamson, D. S., Parratt, M. J., Bower, J. F., Moore, J. D., Richardson, C. M., Dokurno,

P., Cansfield, A. D., Francis, G. L., Hebdon, R. J., Howes, R., Jackson, P. S., Lockie, A. M., Murray, J. B., Nunns, C. L., Powles, J., Robertson, A., Surgenor, A. E. & Torrance, C. J. (2005). *Bioorg. Med. Chem. Lett*. **15**, 863–867.

25. Wu, J. P., Wang, J., Abeywardane, A., Andersen, D., Emmanuel, M., Gautschi, E., Goldberg, D. R., Kashem, M. A., Lukas, S., Mao, W.,Martin, L., Morwick, T., Moss, N., Pargellis, C., Patel, U. R., Patnaude, L., Peet, G. W., Skow, D., Snow, R. J., Ward, Y., Werneburg, B. & White, A. (2007). *Bioorg. Med. Chem. Lett*. **17**, 4664–4669.
26. Wu, S. Y., McNae, I., Kontopidis, G., McClue, S. J., McInnes, C., Stewart, K. J., Wang, S., Zheleva, D. I., Marriage, H., Lane, D. P., Taylor, P., Fischer, P. M. & Walkinshaw, M. D. (2003). *Structure*, **11**, 399–410.

Chapter 3

Structure of the β-form of human MK2 in complex with the non-selective kinase inhibitor TEI-L03090

Summary

Mitogen-activated protein kinase-activated protein kinase 2 (MK2 or MAPKAP-K2), a serine/threonine kinase from the p38 mitogen-activated protein kinase signaling pathway, plays an important role in the production of TNF-α and other cytokines. In a previous report, it was shown that MK2 in complex with the selective inhibitor TEI-I01800 adopts an α-helical Gly-rich loop that is induced by the stable non-planar conformer of TEI-I01800. To understand the mechanism of the structural change, the structure of MK2 bound to TEI-L03090, which lacks the key substituent found in TEI-I01800, was determined. MK2–TEI-L03090 has a β-sheet Gly-rich loop in common with other kinases, as predicted. This result suggests that a small compound can induce a drastic conformational change in the target protein structure and can be used to design potent and selective inhibitors.

1 Introduction

Mitogen-activated protein kinase-activated protein kinase 2 (MK2 or MAPKAP-K2), a Ser/Thr kinase from the p38 mitogen activated protein kinase (p38 MAPK) signaling pathway, plays an important role in the production of TNF-α and other cytokines (Beyaert *et al*., 1996). P38 MAPK signaling plays a role in a variety of inflammatory and other conditions, such as asthma, rheumatoid arthritis, Crohn's disease, atherosclerosis and cancer. Therefore, inhibition of the p38 MAPK pathway is a promising anti-inflammatory drug target (Cuenda & Rousseau, 2007). MK2 is a downstream kinase of p38 MAPK that is directly phosphorylated by p38 MAPK and that has also attracted attention as a target for anti-inflammatory therapy (Gaestel *et al*., 2007; Ronkina *et al*., 2010). In fact, several groups have developed programs for anti-inflammatory therapies by generating MK2 inhibitors and have reported crystal structures of MK2 (Wu *et al*., 2007; Hilling *et al*., 2007; Anderson *et al*., 2007; Anderson, Meyers, Kurumbail, Caspers, Poda, Long, Pierce, Mahoney & Mourey, 2009; Anderson, Meyers, Kurumbail, Caspers, Poda, Long, Pierce, Mahoney, Mourey *et al*., 2009; Revesz *et al*., 2010; Velcicky *et al*., 2010; Argiriadi *et al*., 2009, 2010; Fujino *et al*., 2010; Barf *et al*., 2011; Oubrie *et al*., 2012).

Protein kinases frequently contain a Gly-rich loop with a consensus sequence (Gly-*X*-Gly-*X*-*X*-Gly) in its N-lobe domain. This loop is part of a β-hairpin that connects the β1 and β2 strands and forms a β-sheet structure that interacts with ATP. MK2 also has a Gly-rich loop sequence ^{71}Gly-Leu-Gly-Ile-Asn-Gly^{76} and, with the exception of two structures of complexes with inhibitors, TEI-I01800 (PDB entry 3a2c; Fujino *et al*., 2010) and a 2,4-diaminopyrimidine derivative from Abbott (PDB entry 3ka0; Argiriadi *et al*., 2010), all MK2 complexes deposited in the PDB have a β-sheet Gly-rich loop (β-form).

Protein kinases are key regulators of cell function and constitute one of the largest and most functionally diverse gene families. Kinases are particularly prominent in signal transduction and the coordination of complex functions, in particular the serine/threonine kinase cyclin-dependent kinase 2 (CDK2), which plays a central role in controlling the cell cycle (Tsai

et al., 1991). Furthermore, interference with the cell cycle via inhibition is likely to be an undesirable feature for chronically used anti-inflammatory drugs, such as an MK2 inhibitor. TEI-I01800 is highly potent and selective for significant kinases and has a 177-fold selectivity for MK2 over CDK2 (its IC_{50} values for MK2 and CDK2 are 0.13 and 23 μ*M*, respectively). Furthermore, we have previously reported crystal structures of MK2 and CDK2 in complex with TEI-I01800 (Fujino *et al*., 2010, 2013; Kosugi *et al*., 2012), which revealed that MK2–TEI-I01800 forms an uncommon α-helical Gly-rich loop (α-form) which is induced by the stable conformer of TEI-I01800. On the other hand, CDK2–TEI-I01800 adopted the β-form commonly observed in CDK2 complexes with a small inhibitor. These results suggest that the collision between Leu70 and the *p*-ethoxyphenyl group at the 7-position of TEI-I01800 triggers a structural change in the Gly-rich loop of MK2. Moreover, the 177-fold selectivity for MK2 over CDK2 is caused by favorable interactions between the MK2-specific hydrophobic pocket exposed by the structural change and TEI-I01800.

TEI-L03090, a derivative of this MK2 inhibitor, exhibited a 7.4-fold selectivity for CDK2 over MK2 (its IC_{50} values for MK2 and CDK2 were 4.7 and 0.63 μ*M*, respectively). This inhibitor lacks a functional group at the position corresponding to the *p*-ethoxyphenyl group of TEI-I01800. In order to understand the mechanism of structural change and selectivity, we determined the crystal structure of MK2 in complex with TEI-L03090. Our results show that MK2–TEI-L03090 adopts the β-form, providing a better understanding of the crucial residue required for structural change and selectivity.

2 Materials and Methods

The human MK2 protein was purified using a modified version of our previously described method (Fujino *et al*., 2010). Purified MK2 was concentrated to 5 mg ml^{-1} (0.13 m*M*) and added to TEI-L03090 at a final concentration of 2 m*M*. Co-crystallization experiments of MK2–TEI-L03090 were performed using the hanging-drop vapour diffusion method under the following conditions: 0.1 *M* sodium acetate pH 5.0, 1.6 *M* ammonium sulfate, 200 m*M* sodium chloride and 1.4 m*M* Deoxy Big CHAP. These conditions were modified from those used for MK2–TEI-I01800; Deoxy Big CHAP significantly changed the appearance and the diffraction limit of the crystals. X-ray diffraction data were collected on the BL41XU beamline at SPring-8 at 100 K using 28% sucrose as a cryoprotectant. The MK2–TEI-L03090 complex crystals diffracted to 3.0 Å resolution and belonged to space group $I2_12_12_1$, with unit-cell parameters a = 180.06, b= 179.68, c = 254.10 Å. The crystal contained six monomer molecules in the asymmetric unit, with a Matthews coefficient (V_M) of 4.57 $Å^3$ Da^{-1} and a solvent content (V_{solv}) of 73.1%. The reflection data were processed with *HKL-200*0 (Otwinowski & Minor, 1997) and molecular replacement was performed by *MOLREP* (Vagin & Teplyakov, 2010) from CCP4 (Winn *et al*., 2011) using the MK2–ADP structure (PDB entry 1ny3; Underwood *et al*., 2003) as a search model. Six monomer molecules were found in an asymmetric unit with R = 41.3% and a score of 66.7%. Rigid-body refinement was then performed using *REFMAC* (Murshudov *et al*., 2011). After rigid-body refinement and restrained refinement with NCS constraints, the R and R_{free} factors were 37.7 and 37.6%, respectively. The electron density maps for TEI-L03090 were generated and assigned using *Coot* (Emsley & Cowtan, 2004), and the R and R_{free} factors reduced to 23.8 and 29.1%, respectively. Structure refinement was continued until the R and R_{free} factors were 24.0 and 28.3%, respectively, without NCS constraints. The statistics of data collection and the final structure are summarized in Table 3-1. The atomic coordinates and structure factors have been deposited in the PDB with accession code 3wi6. All figures were produced using *Discovery Studio* (Accelrys Inc.; http://accelrys.com/).

	MK2–TEI-L03090
Data collection	
Beamline	SPring-8 BL41XU
Space group	$I2_12_12_1$
Unit-cell parameters (Å)	
a	180.06
b	179.68
c	254.10
Wavelength (Å)	1.000
Resolution range (Å)	100.00–3.00 (3.11–3.00)
Total No. of reflections	415444
No. of unique reflections	82822
Completeness (%)	99.7 (100.0)
Redundancy	5.0 (5.0)
$\langle I/\sigma(I) \rangle$	13.4 (3.1)
R_{merge}	0.078 (0.434)
Refinement	
Resolution range (Å)	30.00–2.99 (3.07–2.99)
No. of reflections (work)	78593 (5454)
No. of reflections (test)	4132 (246)
R_{work}	0.240 (0.303)
R_{free}	0.283 (0.385)
Total protein atoms	13428
Total ligand atoms	114
Total waters	0
R.m.s.d. from ideal value	

Bonds (Å)	0.019
Angles (°)	1.566
Angles (°)	1.566
Overall average *B*-factor (Å^2)	80.0
Ramachandran plot analysis	
Most favoured regions (%)	91.1
Additionally allowed regions (%)	8.8
Generously allowed regions (%)	0.1
Disallowed regions (%)	0

Table 3-1 Data collection and refinement statistics

Values in parentheses are for the highest resolution shell.

3 Results and discussion

Unlike other reported MK2 crystals, the crystal of MK2–TEI-L03090 belonged to space group $I2_12_12_1$ and contained two trimers in an asymmetric unit (Figs. 3-1 and 3-2).

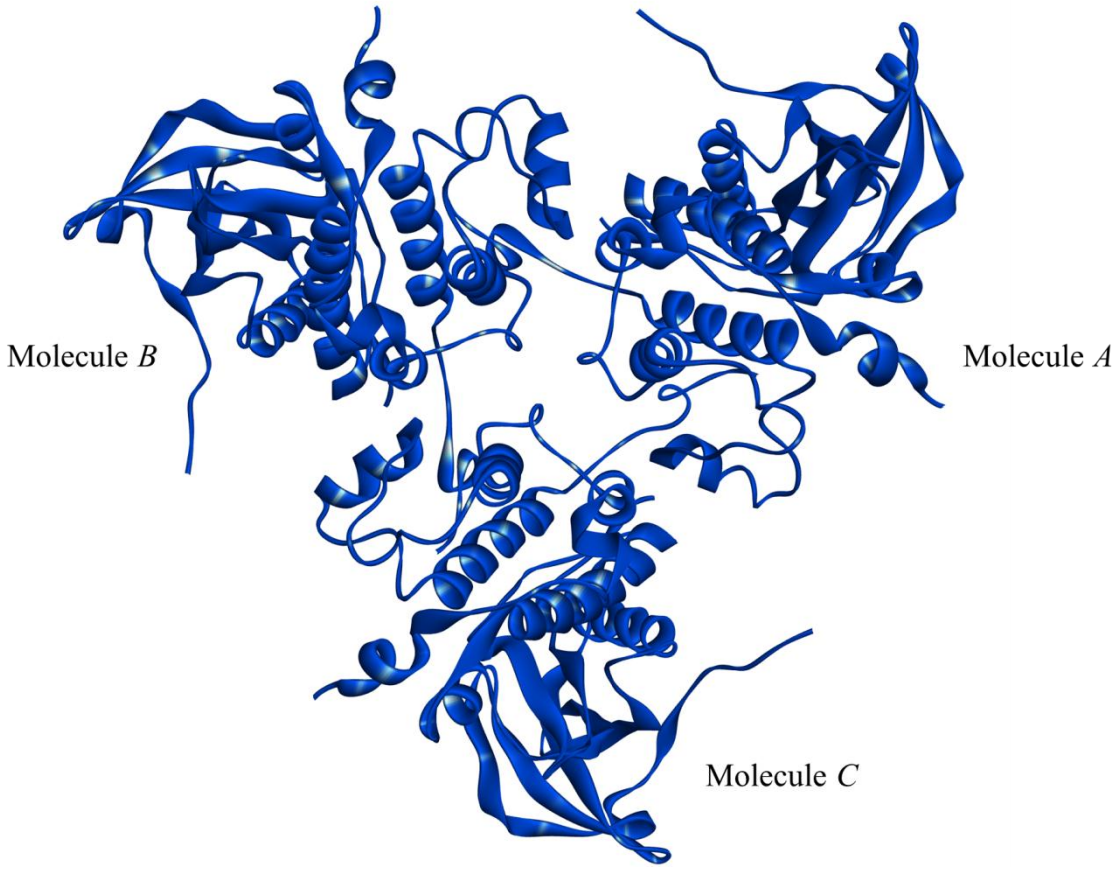

Figure 3-1 A trimer composed of molecules *A*, *B* and *C*.

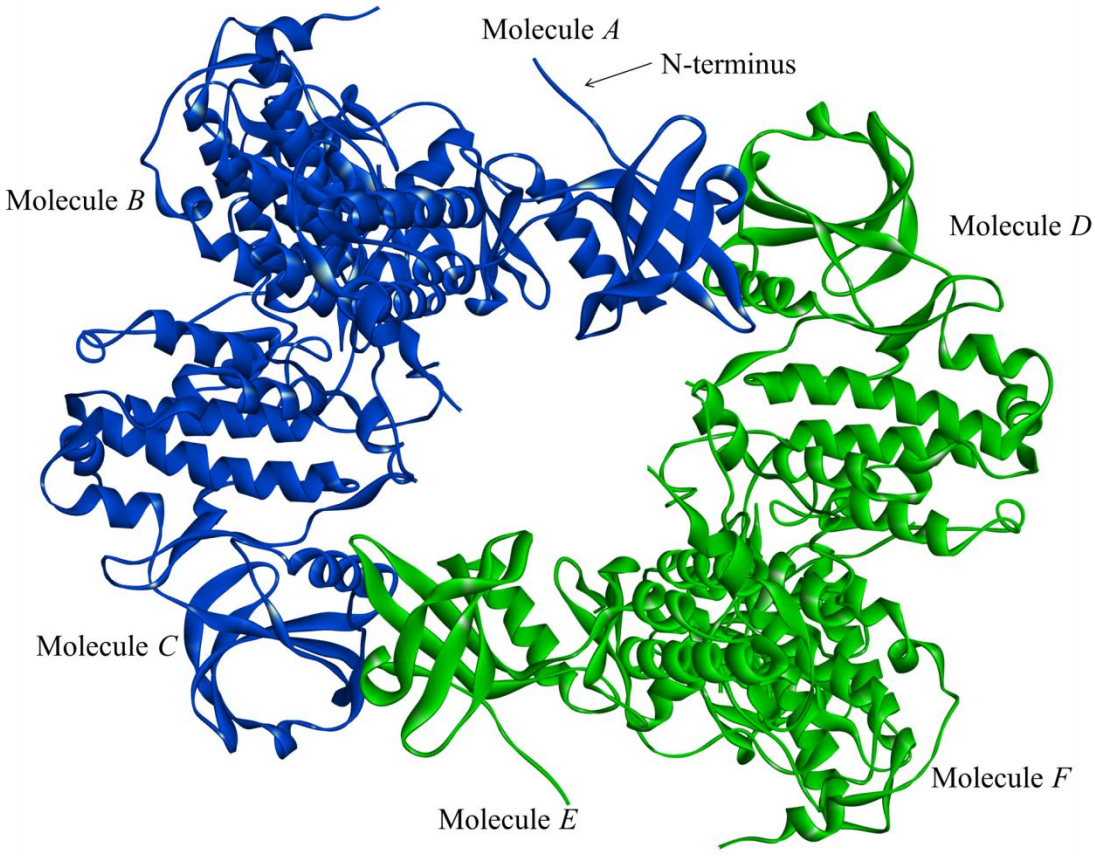

Figure 3-2 The six monomer molecules in the asymmetric unit of MK2.

ABC trimer is shown in blue and *DEF* trimer is shown in green.

Similar to MK2–TEI-I01800, the substrate-binding pocket of molecule *A* interacted with part of a neighboring molecule (molecule *C*, residues 228–235) in the asymmetric unit and the N-terminus interacted with a neighboring molecule related by the 2_1 screw axis. As a result, MK2–TEI-L03090 exhibited a similar oligomerization state, which consisted of 12 molecules of MK2–TEI-I01800. The root-mean-square deviation (r.m.s.d.) on C^{α} atoms between the monomers of MK2–TEI-L03090 is less than 1 Å. Molecule *A*, which had the lowest average *B*-factor, was selected as the monomer structure and is discussed below. The monomer structure of MK2–TEI-L03090 is shown in Fig. 3-3.

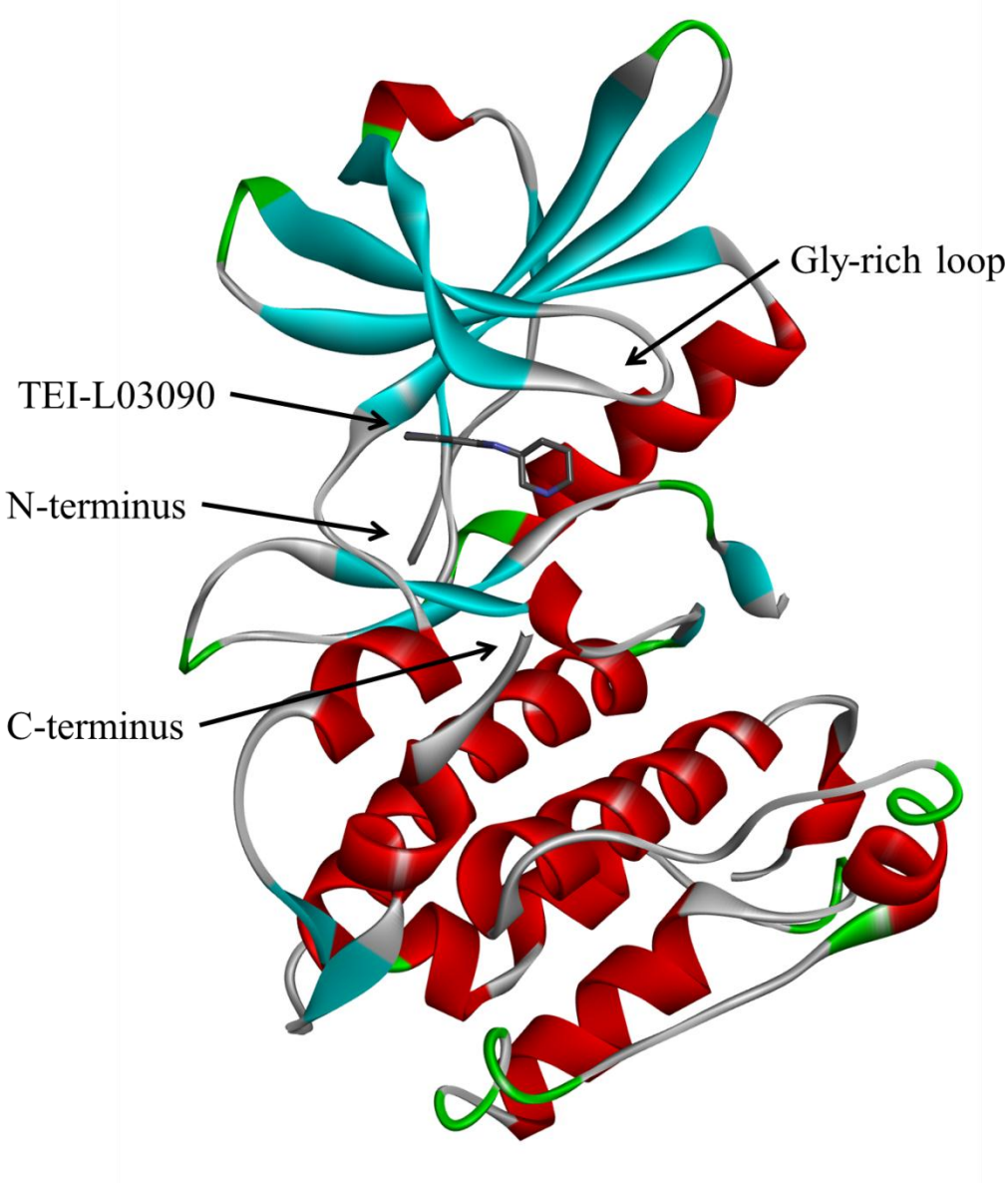

Figure 3-3 Overall structure of MK2–TEI-L03090.

The overall kinase fold of MK2–TEI-L03090 is shown in ribbon representation (α-helices are shown in red, β-sheets in blue and β-turns in green).

Residues 154–156, 217–226, 239–240 and 266–270 were disordered and poor density maps were obtained. TEI-L03090 was bound to the ATP-binding pocket and the Gly-rich loop formed a β-sheet structure similar to that in MK2–ADP (PDB entry 1ny3) and other MK2–inhibitor complexes. The r.m.s.d. on C^{α} atoms between MK2–TEI-L03090 and MK2–ADP was 0.60 Å.

The molecular structure and atomic numbering of TEI-L03090 and TEI-I01800 are shown in Fig. 3-4.

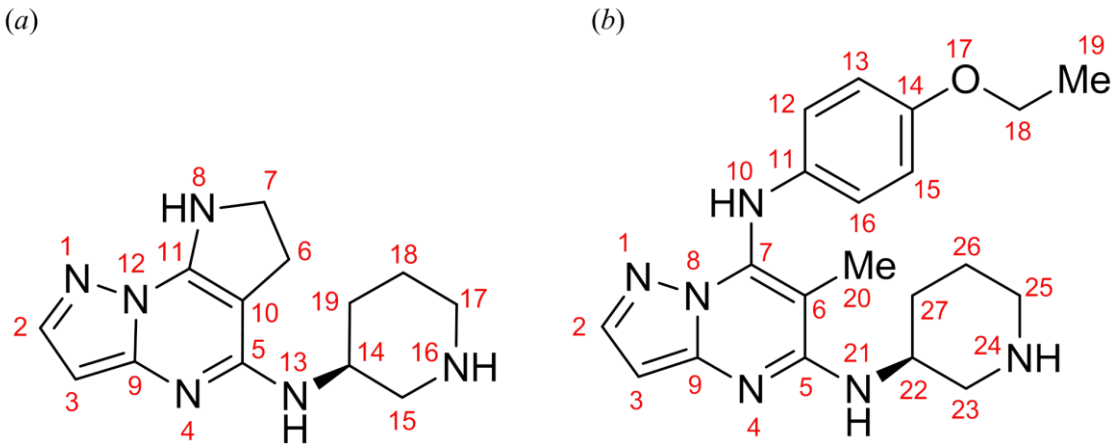

Figure 3-4 Molecular structures of (*a*) TEI-L03090 and (*b*) TEI-I01800.

TEI-L03090 cyclized between the 6- and 7-positions of TEI-I01800 and has a pyrazolo[1,5-*a*]pyrrolo-[3,2-*e*]pyrimidine scaffold with a (3*S*)-piperidylamino group at the 5-position. Its inhibitory activities (IC_{50} values) for MK2 and CDK2 are 4.7 and 0.63 μ*M*, respectively.

The density map and interactions of TEI-L03090 are shown in Fig. 3-5.

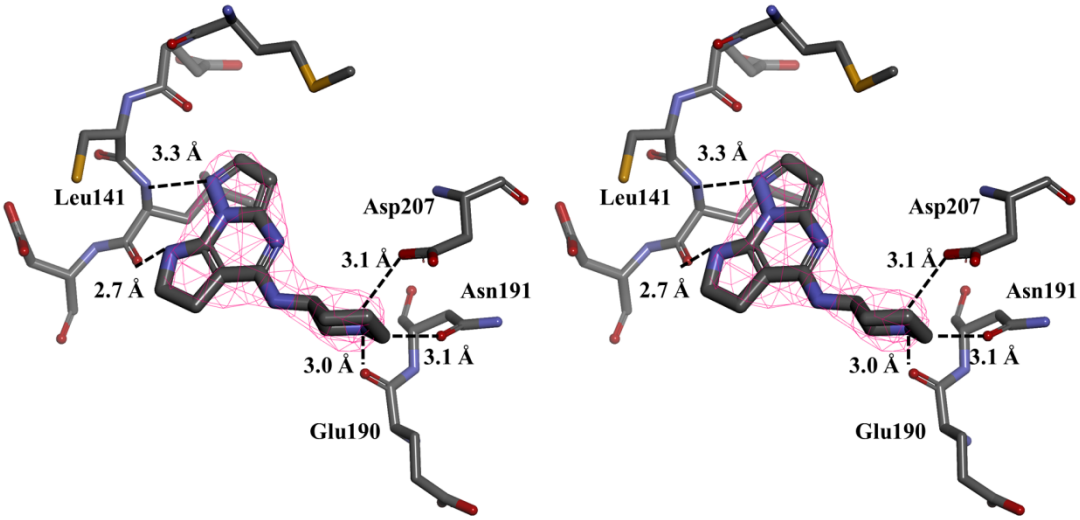

Figure 3-5 Stereo figures of the binding interactions between MK2 and TEI-L03090.

The electron density map of TEI-L03090 is drawn by $F_o - F_c$ OMIT map contoured at 4.0 σ.

TEI-L03090 interacted with the backbone amide of Leu141 through the two hydrogen bonds TEI-L03090 N1—Leu141 N (3.3 Å) and TEI-L03090 N8—Leu141 O (2.7 Å). The N16 atom of TEIL03090 may be ionized and interact with the carbonyl group of Asp207 (3.1 Å), the backbone carbonyl oxygen atom of Glu190 (3.0 Å) and the OD1 atom of Asn191 (3.1 Å).

Fig. 3-6 shows a comparison between the interactions in MK2–TEI-L03090 and MK2–TEI-I01800.

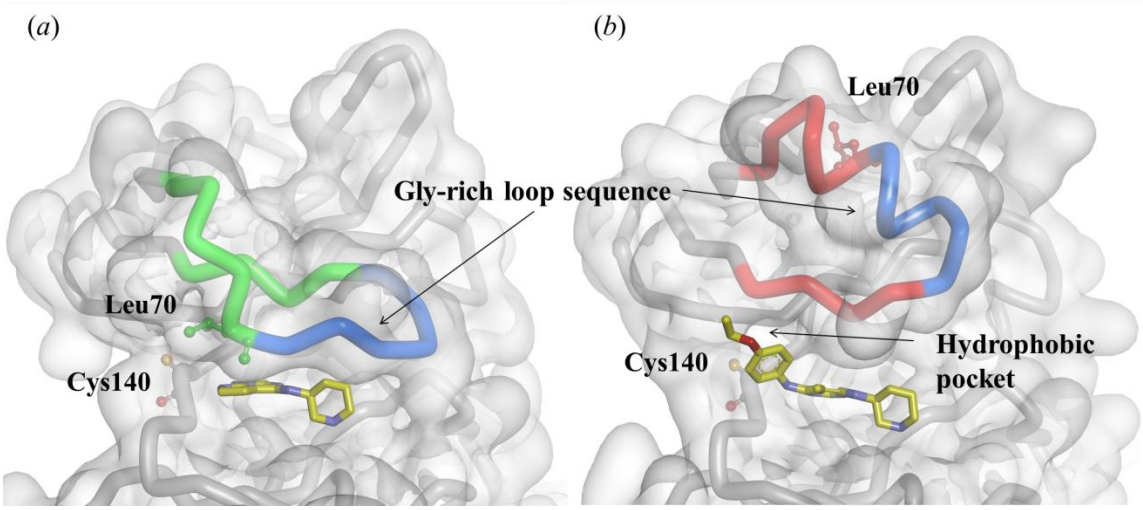

Figure 3-6 Structural comparison of the Gly-rich loops and the key residues Leu70 and Cys140.

(*a*) MK2–TEI-L03090 (β-form of residues ^{65}VTAQVLGLGINGKVLQ^{80} with large conformational changes, green; Gly-rich loop, blue) and (*b*) MK2–TEI-I01800 (α-form of the same residues, red; Gly-rich loop, blue)

Interestingly, TEI-L03090 did not change the conformation of the Gly-rich loop. The average r.m.s.d. between all C^{α} atoms of the two complex structures was 1.96 Å. However, the average r.m.s.d. of the α-form or β-form region, ^{65}VTAQVLGLGINGKVLQ^{80}, which contains the Gly-rich loop sequence, was the largest (6.93 Å). The interactions of TEI-L03090 with Leu141, Glu190, Asn191 and Asp207 were similar to those of MK2–TEI-I01800 (Fig. 3-7).

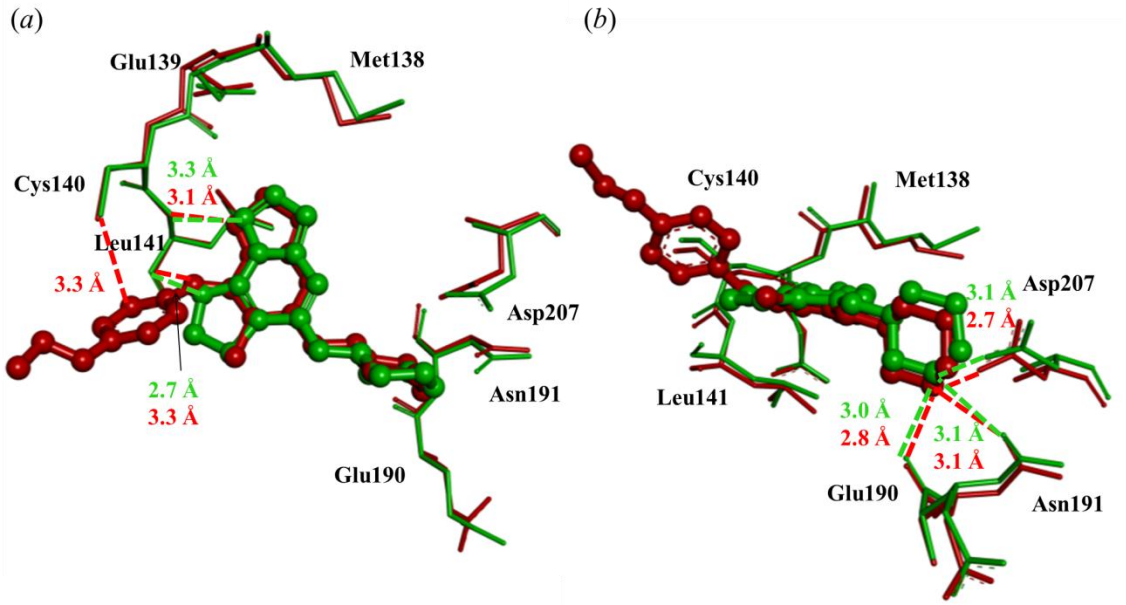

Figure 3-7 Top view (*a*) and side view (*b*) of the binding interactions of MK2 with TEI-L03090 (green) and TEI-I01800 (red).

However, the distances of these hydrogen bonds, with the exception of TEI-L03090 N8—Leu141 O, were longer than those in MK2–TEI-I01800. These long hydrogen bonds could be the reason why TEI-L03090 shows weak inhibition. Furthermore, the interactions between Cys140 and TEI-I01800 are important for MK2 activity, as described in our previous study (Fujino *et al*., 2010, 2013; Kosugi *et al*., 2012). TEI-L03090 lacked van der Waals contacts with Cys140 because TEI-L03090 lacks a substituent at the 8-position corresponding to the *p*-ethyoxyphenyl group at the 7-position of TEI-I01800. The inhibitory activity also decreased in the absence of Cys140 interactions.

In order to bind to Cys140, TEI-I01800 modified the Gly-rich loop of MK2 from the β-form to the α-form because Cys140 is only exposed when this structural change occurs (Fig. 3-6*b*). We speculate that collision between Leu70 and the *p*-ethoxyphenyl group at the 7-position of TEI-I01800 triggers this structural change. The *p*-ethoxyphenyl group at the 7-position is the only structural difference between TEI-I01800 and TEI-L03090. Therefore, the fact that TEI-L03090 does not induce this structural change is consistent with our hypothesis that the structural change is caused by collision of Leu70 and TEI-I01800. TEI-L03090 showed

inhibitory activity for not only MK2 and CDK2 but also other kinases (data not shown), which may be owing to interactions with hinge and phosphate-binding regions that are highly conserved in the kinase family. Moreover, TEI-L03090 is planar because of cyclization between the 6- and 7-positions of TEI-I08000 and can bind the β-form pockets of various kinases. On the other hand, the stable conformer of the selective inhibitor TEI-I01800 was non-planar, favoring the induced α-form pocket over the β-form pocket. Thus, our data also support the high selectivity of TEI-I01800 being a consequence of its characteristic interactions with the α-form of MK2.

4 Conclusion

In this communication, we solved the crystal structure of MK2 in complex with the non-selective inhibitor TEI-L03090, which inhibits MK2, CDK2 and other kinases. MK2 adopts a β-form in this complex, as we predicted because TEI-L03090 lacks a substituent that collides with Leu70 in the Gly-rich loop. These results strongly support the structural change of MK2 from the β-form to the α-form being induced by collisions between Leu70 and TEI-I01800, and this structural change increases its selectivity for MK2 over CDK2. Thus, our research suggests that a small compound can induce a drastic conformational change in a target protein structure, and this phenomenon may be useful in developing potent and selective inhibitors.

References

1. Anderson, D. R., Meyers, M. J., Kurumbail, R. G., Caspers, N., Poda, G. I., Long, S. A., Pierce, B. S., Mahoney, M. W. & Mourey, R. J. (2009). *Bioorg. Med. Chem. Lett*. **19**, 4878–4881.
2. Anderson, D. R., Meyers, M. J., Kurumbail, R. G., Caspers, N., Poda, G. I., Long, S. A., Pierce, B. S., Mahoney, M. W., Mourey, R. J. & Parikh, M. D. (2009). *Bioorg. Med. Chem. Lett*. **19**, 4882–4884.
3. Anderson, D. R., Meyers, M. J., Vernier, W. F., Mahoney, M. W., Kurumbail, R. G., Caspers, N., Poda, G. I., Schindler, J. F., Reitz, D. B. & Mourey, R. J. (2007). *J. Med. Chem*. **50**, 2647‑2654.
4. Argiriadi, M. A., Ericsson A. M., Harris C. M., Banach D. L., Borhani D. W., Calderwood D. J., Demers M. D., Dimauro J., Dixon R. W., Hardman J., Kwak S., Li B., Mankovich J. A., Marcotte D., Mullen K. D., Ni B., Pietras M., Sadhukhan R., Sousa S., Tomlinson M. J., Wang L., Xiang T., Talanian R. V. (2010). *Bioorg. Med. Chem. Lett*. **20**, 330–333.
5. Argiriadi, M. A., Sousa S., Banach D., Marcotte D., Xiang T., Tomlinson M. J., Demers M., Harris C., Kwak S., Hardman J., Pietras M., Quinn L., DiMauro J., Ni B., Mankovich J., Borhani D. W., Talanian R. V., Sadhukhan R. (2009). *BMC Struct. Biol*. **9**, 16.
6. Barf, T., Kaptein , A., de Wilde, S., van der Heijden , R., van Someren , R., Demont , D., Schultz-Fademrecht , C., Versteegh , J., van Zeeland , M., Seegers , N., Kazemier, B., van de Kar , B., van Hoek, M., de Roos, J., Klop , H., Smeets, R., Hofstra , C., Hornberg , J. & Oubrie , A. (2011). *Bioorg. Med. Chem. Lett*. **21**, 3818–3822.
7. Beyaert, R., Cuenda, A., Vanden Berghe, W., Plaisance, S., Lee, J. C., Haegeman, G., Cohen, P. & Fiers, W. (1996). *EMBO J*. **15**, 1914–1923.
8. Cuenda, A. & Rousseau, S. (2007). *Biochim. Biophys. Acta*, **1773**, 1358‑1375.
9. Emsley, P. & Cowtan, K. (2004). *Acta Cryst*. D**60**, 2126–2132.
10. Fujino, A., Fukushima, K., Kubota, T., Kosugi, T. & Takimoto-Kamimura, M. (2013). *J. Synchrotron Rad*. **20**, 905–909.

11. Fujino, A., Fukushima, K., Namiki, N., Kosugi, T. & Takimoto-Kamimura, M. (2010). *Acta Cryst*. D**66**, 80–87.
12. Gaestel, M., Mengel, A., Bothe, U. & Asadullah, K. (2007). *Curr. Med. Chem*. **14**, 2214–2234.
13. Hillig, R. C., Eberspaecher, U., Monteclaro, F., Huber, M., Nguyen, D., Mengel, A., Muller-Tiemann, B. & Egner, U. (2007). *J. Mol. Biol*. **369**, 735–745.
14. Kosugi, T., Mitchell, D.R., Fujino, A., Imai, M., Kambe, M., Kobayashi, S., Makino, H., Matsueda, Y., Oue, Y., Komatsu, K., Imaizumi, K., Sakai, Y., Sugiura, S., Takenouchi, O., Unoki, G., Yamakoshi, Y., Cunliffe, V., Frearson , J., Gordon, R., Harris, C.J., Kalloo-Hosein H., Le J., Patel G., Simpson D. J., Sherborne B., Thomas P. S., Suzuki N., Takimoto-Kamimura M., Kataoka K. (2012). *J. Med. Chem*. **55**, 6700–6715.
15. Murshudov, G. N., Skubák, P., Lebedev, A. A., Pannu, N. S., Steiner, R. A., Nicholls, R. A., Winn, M. D., Long, F. & Vagin, A. A. (2011). *Acta Cryst.* D**67**, 355–367.
16. Otwinowski, Z. & Minor, W. (1997). *Methods Enzymol*. **276**, 306–327.
17. Oubrie, A., Kaptein, A., de Zwart, E., Hoogenboom, N., Goorden, R., van de Kar, B., van Hoek, M., de Kimpe, V., van der Heijden, R., Borsboom, J., Kazemier, B., de Roos, J., Scheffers, M., Lommerse, J., Schultz-Fademrecht, C., Barf, T. (2012). *Bioorg. Med. Chem. Lett.* **22**, 613–618.
18. Revesz, L., Schlapbach, A., Aichholz, R., Dawson, J., Feifel, R., Hawtin, S., Littlewood-Evans, A., Koch, G., Kroemer, M., Möbitz, H., Scheufler, C., Velcicky, J., Huppertz, C. (2010). *Bioorg. Med. Chem. Lett.*, **20**, 4719–4723.
19. Ronkina, N., Menon, M. B., Schwermann, J., Tiedje, C., Hitti, E., Kotlyarov, A. & Gaestel, M. (2010). *Biochem. Pharmacol*. **80**, 1915–1920.
20. Tsai, L.-H., Harlow, E. & Meyerson, M. (1991). *Nature (London)*, **353**, 174–177.
21. Underwood, K. W. et al. (2003). *Structure*, **11**, 627–636.
22. Vagin, A. & Teplyakov, A. (2010). *Acta Cryst*. D**66**, 22–25.
23. Velcicky, J., Feifel, R., Hawtin, S., Heng, R., Huppertz, C., Koch, G., Kroemer, M., Moebitz, H., Revesz, L., Scheufler, C. & Schlapbach, A. (2010). *Bioorg. Med. Chem. Lett*.

20, 1293–1297.

24. Winn, M. D. et al. (2011). *Acta Cryst.* D**67**, 235–242.
25. Wu, J.-P., Wang J., Abeywardane A., Andersen D., Emmanuel M., Gautschi E., Goldberg D. R., Kashem M. A., Lukas S., Mao W., Martin L., Morwick T., Moss N., Pargellis C., Patel U. R., Patnaude L., Peet G. W., Skow D., Snow R. J., Ward Y., Werneburg B., White A.. (2007). *Bioorg. Med. Chem. Lett*. **17**, 4664–4669.

Overall Conclusion

In this thesis, we demonstrated that TEI-I01800 which is a small molecule MK2 inhibitor changed the Gly-rich loop of MK2 from β-sheet to α-helix because of the collision between the *p*-ethoxyethyl group at the 7-position of TEI-I101800 and Leu70. Moreover, the *p*-ethoxyethyl group at the 7-position of TEI-I101800 is bound to MK2 with specific interaction to Cys140 exposed by this structural change. This structural change also induced the binding pocket to a favorable shape. Our hypothesis about the structural change mechanism of MK2 in complex with TEI-I01800 was strongly supported by the MK2–TEI-L03090 complex structure with the β-sheeted Gly-rich loop. Because TEI-L03090 lacks the *p*-ethoxyphenyl group from TEI-I01800, it is impossible to change the Gly-rich loop of MK2. The mechanism of kinase selectivity of TEI-I01800 was indicated by the structure of CDK2–TEI-I01800 complex. The stable and non-planar conformation of TEI-I01800 can only bind to the α-form specific binding pocket induced by the TEI-I01800 and shows good potency for MK2. However it cannot bind to the narrow binding pocket of β-form CDK2.

In the drug discovery research, the structures of target protein in complex with inhibitors are very important to understand the binding interaction and to design more potent inhibitors. Usually, we start the development of inhibitors from the initial hit ligands found by the compound library using bioassay as called high throughput screening (HTS). However, the hit ratio of HTS from the large library which consisted of 100,000 to 1 million compounds is very low (about 0.01%). In order to improve the hit ratio, we attempt to design the small molecule library called as focused library using ligand based drug design (LBDD), structure based drug design (SBDD) and fragment based drug design (FBDD) and so on, in the results, the hit ratio can be improved from several percent to several 10%. If the structure of target protein is known, SBDD or FBDD is very useful for drug screening. In such screening, the target protein structure is defined as fixed conformation because of the calculation speed or the complex methods. On the other hand, it is known that the protein structure is very flexible and has plasticity, then, the protein undergoes an induced-fit conformational change by its ligand. Thus, if the several

complex structures are known, it is important to understand the binding mechanism and use these structures effectively for finding the novel inhibitors.

Once the initial hit compounds are found, we try to solve the crystal structure in complex with them in order to determine the actual binding site and binding interaction between protein and ligand. Because it is very difficult to predict the structure induced by the specific ligand before the structure determination, determination of the complex structures with several initial hit compounds that have different or unique scaffolds with attractive activities is significant. If the ligands that can change the target protein are found, the possibility for designing the potent and selective inhibitor would be increased as shown by our results. Actually, although we could not predict the α-form MK2 before the structure determination, once the structure was revealed the strategies for increasing the potency and selectivity were clearly defined.

Here, we show one possibility for obtaining the compound which may cause such a structural change based on the structure analysis of MK2. The native apo–MK2 and MK2–AMP-PNP complex structure, which have been preliminarily determined in our laboratory (data not shown) showed the β-form structure and MK2–ADP (PDB code 1ny3) also has β-form structure. These ligands are ATP homologues and the scaffolds are very similar to substrate ATP (Fig. 0-4).

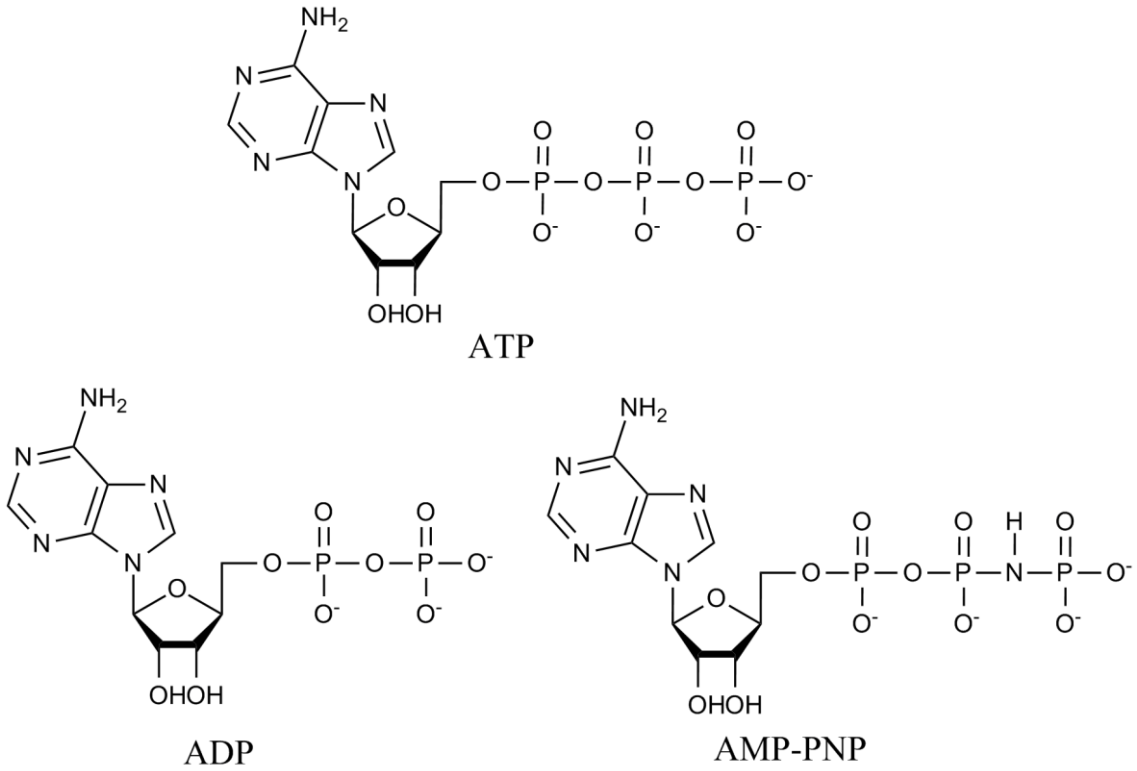

Figure 0-4 Molecular structure of ATP and its analogues.

The reason why such substrate analogues does not undergo the induced-fit like TEI-I01800 is that substrate analogue does not have efficient volume or key substituent needed to structural change. The substrate analogues or small molecule inhibitors that can bind to the protein without the structural change are good starting points of inhibitor design, but the inhibitory activities are very weak compared with the drug-like ligands, so the transformation of the scaffold called as scaffold hopping and the modification and addition of substituents for more potent inhibition. Moreover, to adopt the structural change, we should try to add the large substituents which may be impossible to be accommodated in the binding pocket.

Below is the case where the substrate analogue did not induce a large structural change. We have previously reported the crystal structure of 1-aminocyclo propane 1-carboxylate deaminase (ACCD) homolog protein from *pyrococcus hosikosii OT3* (phAHP) in complex with its substrate analogue inhibitor ACC (Fig. 0-5).

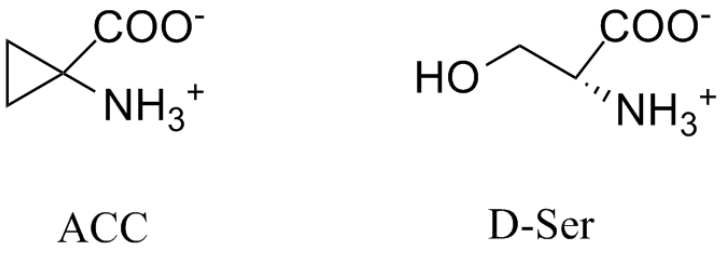

ACC D-Ser

Figure 0-5 Molecular structures of ACC (substrate homologue) and D-ser (substrate).

As shown in Fig. 0-6, in the complex structure of phAHP–ACC, we found the conformational change which makes the small domain of phAHP close to the large domain (domain closure) because of the binding of ACC in the substrate pocket between the small and large domain.

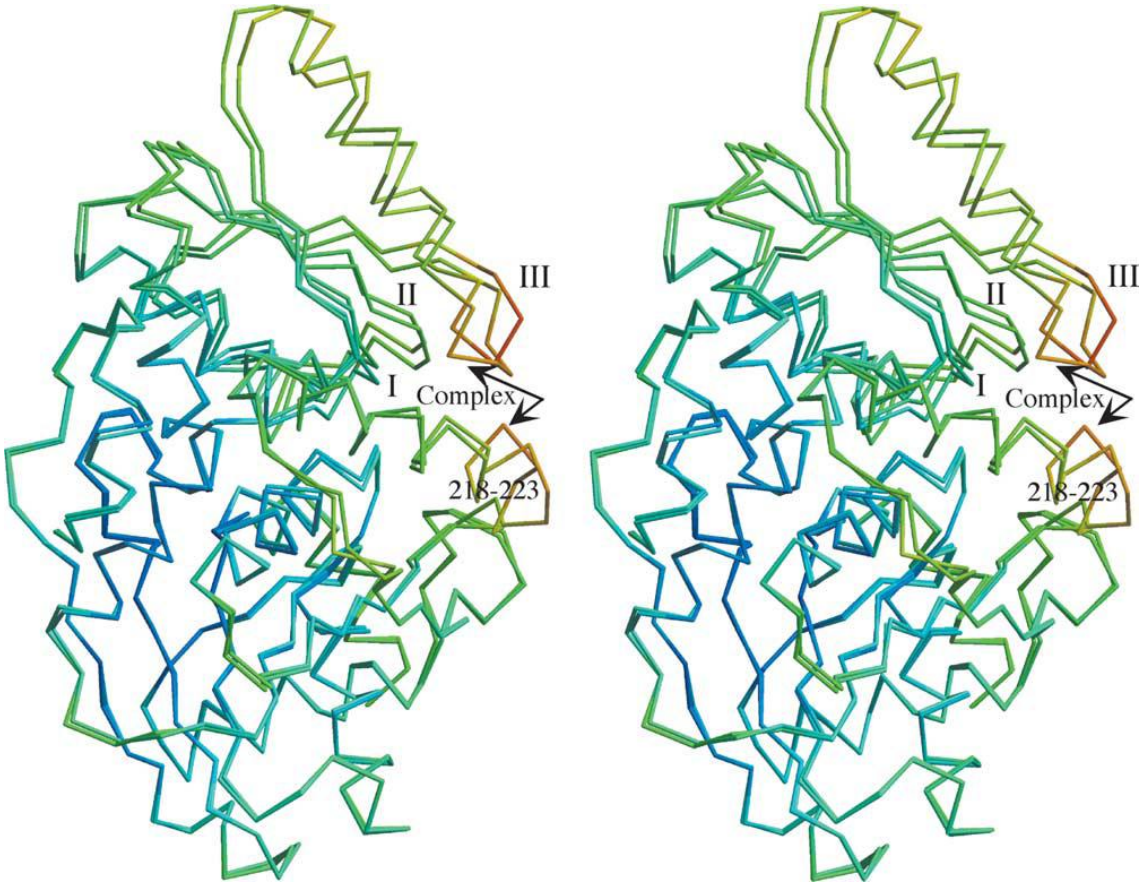

Figure 0-6 Stereo view showing the comparison between apo–phAHP and phAHP–ACC.

The ACC complexed structure is indicated by arrows in the Figure. The C^{α} trace modes are colored according to the *B*-factor by a rainbow color ramp from red at the highest *B*-factor values to blue at the lowest *B*-factor value regions. The regions I, II, and III indicate the portion with higher *B*-factor explained in the text and for Fig. 0-7.

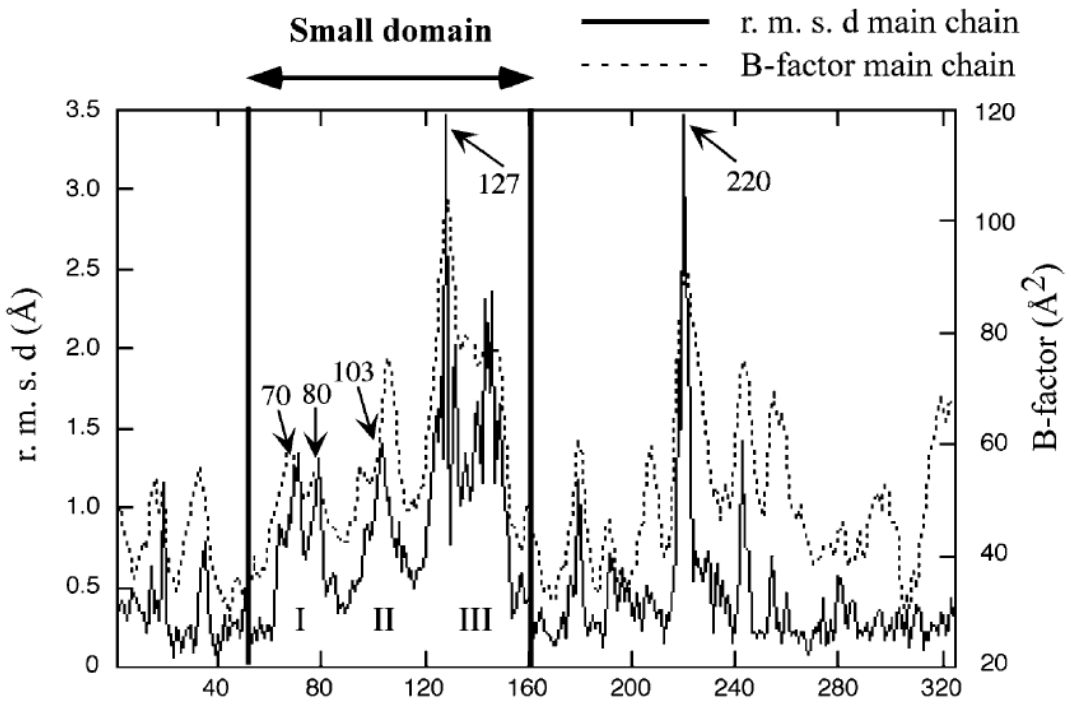

Figure 0-7 R.m.s.d. and *B*-factor plot versus amino-acid residue numbers.

A continuous line represents the r.m.s.d. score of the main-chain between apo–phAHP and phAHP–ACC and a dotted line represents the main-chain *B*-factor value of the apo–phAHP structure.

The maximum r.m.s.d. of main chain atom between apo–phAHP and phAHP–ACC is about 3.5 Å (Fig. 0-7) and it is also demonstrated that the protein structure is flexible and could be induced by the ligand binding. However the drastic secondary structural change observed in the MK2–TEI-I01800 was not found in phAHP–ACC. Because ACC is a substrate analogue of phAHP and the structure is very similar to substrate D-Ser (Fig. 0-5), the large conformational change might not be adopted. From these results it can be concluded that, in order to obtain a potent and selective inhibitor like TEI-I01800, it is required for a substrate or a small fragment to add the characteristic substituent group which expands the substrate pocket and causes the large structural change in target protein.

As above, in this thesis, we demonstrated the importance of the determination of protein-ligand complex structure and the use of the structural change induced by the

characteristic ligand to design the potent and selective inhibitors. This thesis is based on the contents of the following publication.

1. Structural analysis of an MK2–inhibitor complex: insight into the regulation of the secondary structure of the Gly-rich loop by TEI-I01800
   Aiko Fujino-Nakajima, Kei Fukushima, Naoko Namiki, Tomomi Kosugi and Midori Takimoto-Kamimura
   Acta Cryst. (2010). D**66**, 80–87

2. Crystal structure of human cyclin-dependent kinase-2 complex with MK2 inhibitor TEI-I01800: insight into the selectivity
   Aiko Fujino-Nakajima, Kei Fukushima, Takaharu Kubota, Tomomi Kosugi and Midori Takimoto-Kamimura
   J. Synchrotron Rad. (2013). **20**, 905–909

3. Structure of the β-form of human MK2 in complex with the non-selective kinase inhibitor TEI-L03090
   Aiko Fujino-Nakajima, Kei Fukushima, Takaharu Kubota, Yoshiyuki Matsumoto and Midori Takimoto-Kamimura
   Acta Cryst. (2010). F**69**, 1344–1348

4. Structural and Enzymatic Properties of 1-Aminocyclopropane-1-carboxylate Deaminase homologue from Pyrococcus horikoshii
   Aiko Fujino-Nakajima, Toyoyuki Ose, Min Yao, Tetsuo Tokiwano, Mamoru Honma, Nobuhisa Watanabe and Isao Tanaka
   J. Mol Biol. (2004). **341**, 999–1013

5. Reaction intermediate structures of 1-aminocyclopropane-1-carboxylate deaminase: insight into PLP-dependent cyclopropane ring-opening reaction.
Toyoyuki Ose, Aiko Fujino-Nakajima, Min Yao, Nobuhisa Watanabe, Mamoru Honma and Isao Tanaka
J. Biol Chem. (2003). **278**, 41069–41076

Acknowledgement

First of all, I wish to express my sincere gratitude to Professor Isao Tanaka and Professor Min Yao, for their cordial guidance, advice, discussion and encouragement. I sincerely thank their helpful support which continues from school days.

Further, I would like to express my gratitude and appreciation to Dr. Midori Takimoto-Kamimura of Teijin Pharma Ltd., for her helpful guidance, suggestion, advice and ceaseless encouragement throughout this work. My research in Teijin Pharma Ltd. is deeply influenced by her insights into drug discovery and chemistry.

I am grateful to Dr. Kenichiro Kataoka, a chief of Teijin Institute for Bio-medical Research, Dr. Kazuya Takenouchi, a head of Medicinal Chemistry Research Laboratories and Mr. Yoshiyuki Matsumoto, a leader of Medicinal Chemistry Technology Group for having given the opportunity of this research.

I also wish to express my thanks to Mr. Tomomi Kosugi, Mr. Yoshiyuki Matsumoto and a lot of medicinal chemists who synthesized MK2 inhibitors.

I would like to appreciate the support on the biological experiments of all the biologists who were related to MK2 project.

I also thank Ms. Naoko Namiki, Mr. Takaharu Kubota, Mr. Masaharu Koizumi, Mr. Kei Fukushima and Dr. Shinji Kakuda for the protein preparation and helpful discussion about X-ray crystallography.

I also wish to express my thanks to all staff of SPring-8 BL32B2 and BL41XU.

Furthermore, I would like to thank a lot of colleagues in Teijin Pharma Ltd., I Tanaka's, M. Yao's and M. Homma's Laboratory.

Finally, I really appreciate powerful supports of my family; Ryota, Yuta, Keita Nakajima and a new life.

Aiko Fujino-Nakajima

December, 2013